Solar Flares and Magnetospheric Particles: Investigations Based Upon the ONR-602 and ONR-604 Experiments

Performance Report

ONR Grant

N00014-90-J-1466

First Quarter FY93

John P. Wefel and T. Gregory Guzik

Department of Physics and Astronomy
Louisiana State University
Baton Rouge, LA 70803-4001

Phone: 504-388-8696
FAX: 504-388-1222

15 February 1993

"Solar Flares and Magnetospheric Particles: Investigations Based Upon the ONR-602 and ONR-604 Experiments"

I. Introduction:

This performance report covers work accomplished under ONR Grant N00014-90-J-1466 related to the radiation environment in near-Earth space. The goal of the research is to measure and describe, quantitatively, the Geospace radiation environment in which men and spacecraft must survive and function. The tools for this investigation are the data returned by the ONR-602 and ONR-604 experiments, both flown under the auspices of ONR and the Air Force Space Test Program, augmented by correlative databases of both space-based and ground-based data. The investigation involves data analysis, modeling and applications to a variety of space equipment and environments.

This report follows the detailed Technical Report that was submitted during Fall, 1992 and builds upon the base established by our previous work. For the current period, the principal effort was in (1) understanding the polar cap access of solar energetic particles, and polar cap structures, during the S81-1 mission (ONR-602 data), and (2) predicting the environment, both from Galactic and Solar particles encountered during the CRRES mission (ONR-604 data).

II. Particle Access over the Polar Caps:

The S81-1 satellite was launched into a low-altitude (170-280 km), polar (inclination = 96.3°), and sun-synchronous (10:30 - 22:30) orbit, gravity gradient stabilized, for studies of energetic electrons and ions (LPARL experiment) and for investigations of solar, magnetospheric, and galactic cosmic rays by the ONR-602 experiment from the Laboratory for Astrophysics and Space Research (LASR) at the University of Chicago. One component of ONR-602, the Monitor telescope, was identical to the Low Energy Telescope (LET) in the University of Chicago cosmic ray experiment on IMP-8 and, together, they provided comparable and simultaneous measurements of MeV protons inside and outside the magnetosphere for studies of solar particle entry processes. The Monitor telescope had a single, passively shielded detector for integral counting rate measurements of protons at 0.6-9 MeV, alphas at 0.8-4.5 MeV/nucleon, and heavier ions at 1-10 MeV/nucleon.

The ONR-602 Main Telescope measured higher energy heavy ions and included position-sensing detectors which provided particle incidence directions within a few degrees in local pitch angle. The Main Telescope included multiple solid state detectors for dE/dx vs. residual E measurements of He-Ni energetic nuclei at 4-230 MeV/nucleon. Pulse height event processing in the Main Telescope was triggered by coincident detector firings corresponding to three priority levels: P3 for >He ions above 4 MeV/nucleon, P2 for >Li above 6 MeV/nucleon, and P1 for >Ne above 13 MeV/nucleon. The ONR-602 sensors had front apertures of 40° (Main Telescope) and 37.7° (Monitor) in conical half angle. The maximum pitch angle response was about 50° in the polar cap regions. Since the S81-1 satellite carried no magnetometer, the magnetic field along the orbit was modeled with a combination of the 1980 IGRF internal and Tsyganenko (1987) external field models.

Solar energetic particle (SEP) entry into the magnetosphere can be divided into two distinctly different access regions: High Polar Latitudes (HPL) and Low Polar Latitudes (LPL). These contiguous regions are divided at geomagnetic latitudes of about 75°, above which the open polar cap field lines (HPL) extend deep into the magnetotail. Below 75°, the LPL encompasses the equatorward transition onto closed field lines and has an equatorward boundary at field lines mapping to the earthward termination of the magnetospheric plasma sheet in the nightside tail

region. Experimentally, the HPL is defined by a flat intensity profile across each polar cap for solar electrons, indicating free and unimpeded access from interplanetary space. In contrast, low energy auroral electrons, and directly penetrating or quasi-trapped SEP particles, may co-exist in the LPL region, which includes the auroral oval zone.

SEP proton profiles across the polar caps may either be flat at high latitudes, like those for electrons, or else show sharp spatial variations in terms of peaks and troughs at various invariant magnetic latitudes and local times. Such variations appear at order of magnitude levels in the proton profiles when the interplanetary proton flux is highly anisotropic during early phases of intensity increases at 1 A.U. from flares which are well-connected along interplanetary magnetic field (IMF) lines from the Sun.

The introduction of position-sensing detectors into energetic particle measurements makes possible precise knowledge of the arrival trajectories for individual SEP ions and pitch angle distributions. Measurement of an ion's energy, mass, and velocity direction allows numerical reconstruction of the ion's entry path through the magnetosphere to the polar cap, if the magnetospheric models are accurate enough to describe the fields affecting the particle's motion. The ONR-602 instrument is capable of such measurements in the Main Telescope, and we have been working to use the data to provide a fresh attack on this problem.

In order to study solar energetic ion access into a relatively unperturbed magnetosphere, a period was selected during a rapid intensity increase of SEP's from a west limb flare. One such flare occurred at N16W89 and commenced on July 22, 1982 at 1649 UT with optical (1F), x-ray (M4), and type II radio burst emissions, followed by a low energy proton increase at about 2000 UT as shown in Figure 1. The ONR-602 ML (polar cap averaged) and IMP-8 LET rate L1NL2 (hourly averaged), both measuring protons >0.6 MeV, are shown along with the ONR-602 Main Telescope P3 rate (nominally helium >4 MeV/nucleon) for one day centered upon the peak intensity of the particle event. Note that ML and L1NL2 track nicely before the event, but the L1NL2 falls below the ML rate during the intense part of the event. Also, indicated in Figure 1 is the solar wind speed and the K_p index during this period. Both the solar wind and K_p are at minimal levels, indicating a relatively quiescent magnetosphere. (Shocked solar wind from the flare did not arrive at Earth until one day after the energetic particle onset.) Note also the points marked 1171 N and 1171 S. These indicate the N and S polar cap crossings that have been investigated in detail.

Figure 2 shows our highest time resolution data (each four-second rate accumulation interval corresponding to 0.5 km of orbital motion) for solar proton and helium counting rates over the north (left) and south (right) polar caps, and down in latitude to the cutoff regions. The times of Stormer cutoff for the proton (>0.5 MeV) and helium (>4 MeV/nucleon) threshold energies are shown for corresponding rigidity cutoffs of 30 MV and 173 MV, respectively, as calculated by $R_c = 14.9/L^2$ GV for a simple internal dipole field. The proton cutoffs are located near the nominal LPL-HPL region boundary at ~75°.

Also shown are the local pitch angles of individual helium and heavier ion events analyzed by the Main Telescope, along with the corresponding pitch angle of the sensor centerline. The finite opening angle of the instrument aperture is manifest in the shift of measured ion pitch angles towards larger values as the boresight moved more than 20° away from the local field direction, hardly any such variations being apparent for smaller boresight angles. S81-1's closest approach to the north and south geomagnetic poles occurred in this orbit at about 85° magnetic latitude on the dawn and dusk sides of the poles, respectively, the times of closest approach being close to the times at which boresight angle reached its minimum value in Figure 2.

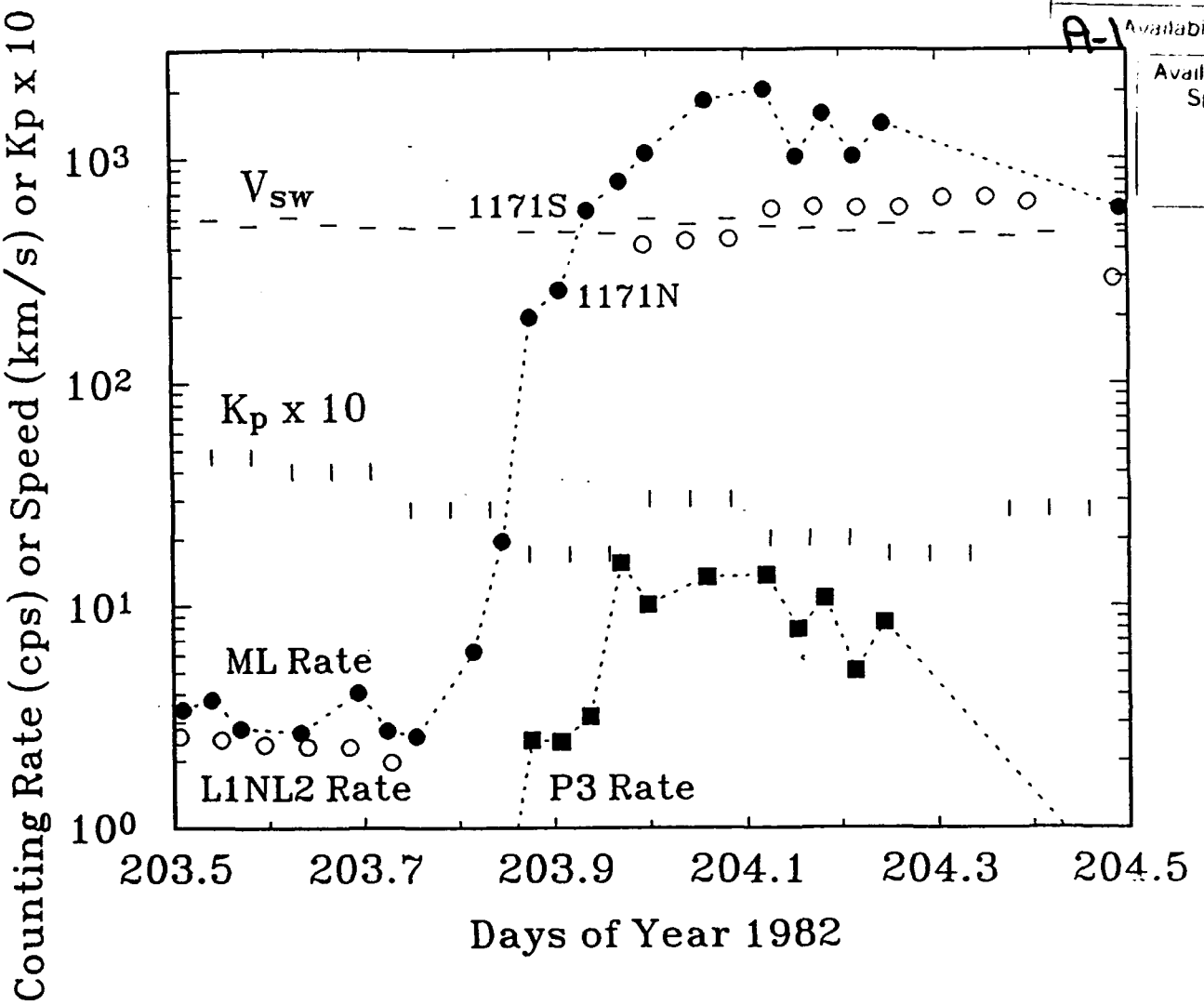

Figure 1. Counting rates for polar cap (ML rate: ●) and interplanetary (IMP-8 L1NL2 rate: O) protons above 0.6 MeV, and helium ions (P3 rate: ■) above 4 MeV/nucleon, during the twelve hours preceding and following the peak intensity as seen at S81-1. The ONR-602 data are averaged over the HPL region above 75° latitude for each polar crossing. Geomagnetic Kp indices and solar wind velocities are shown. S81-1 orbit numbers, and N or S for the respective poles, are given for selected points.

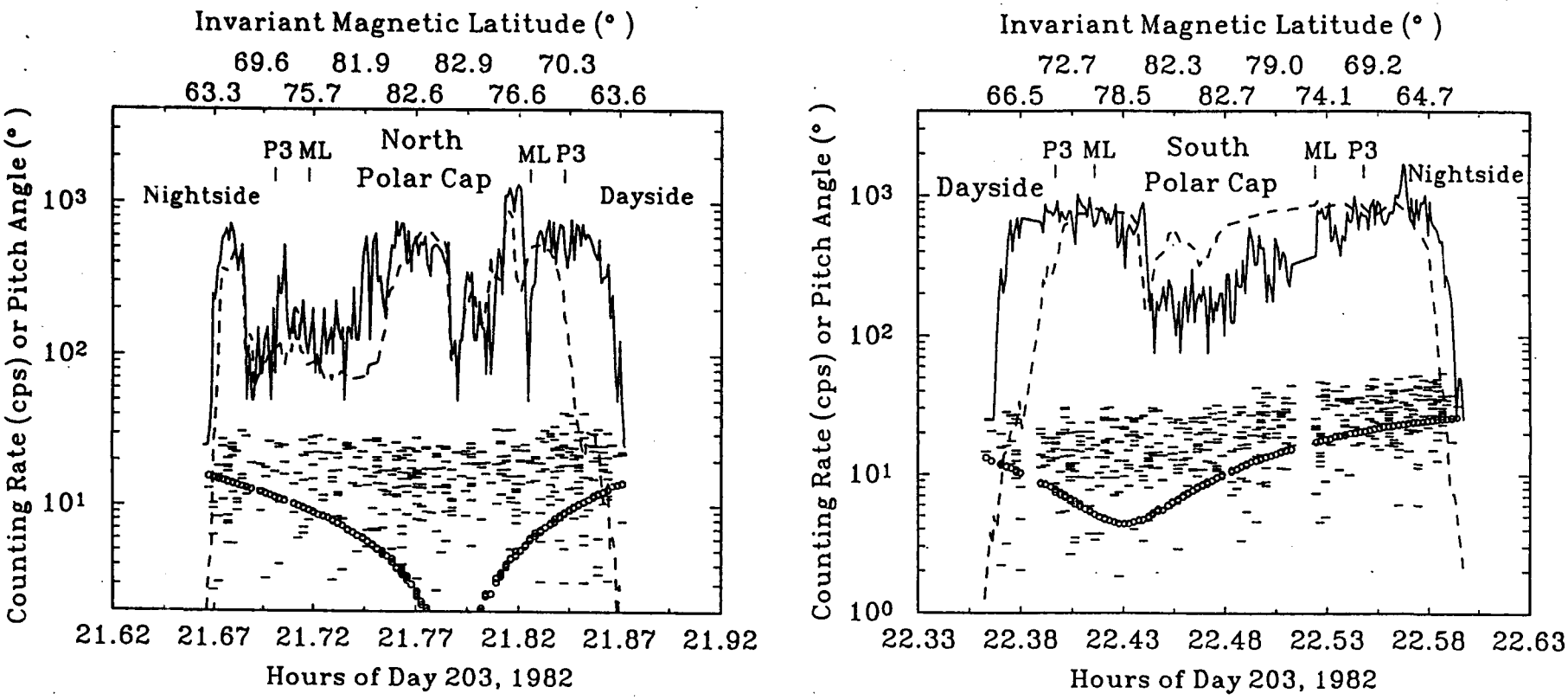

Figure 2: Proton (ML rate: dashed curve) and helium (P3 rate x 100: solid curve) counting rates measured across the northern (left) and southern (right) polar caps during orbit 1171 on 22 July (day of year 203) between the dayside and nightside cutoff regions. Also shown are the calculated vertical cutoff positions (|) at the threshold energies for protons (ML) and helium (P3). Pitch angles of the main telescope boresight (O) and incident ions (—) are plotted, on the same numerical scale as the counting rates, for each analyzed helium event. Minimal boresight pitch angles indicate closest proximity to the magnetic pole for each polar crossing.

In general, the range of pitch angles showed no significant correlations to sudden changes in counting rates, except that more ions were analyzed during some intervals of higher rates. The lack of any pitch angle shift correlated to the rate change indicates that the rate variations were not due to changes in anisotropy of penetrating ions which would affect access of SEP ions from the magnetopause. Also, there were no significant pitch angle changes at ~75° magnetic latitude as might otherwise be expected from moving into particle populations dominated by quasi-trapped ions. The distinction between LPL and HPL is non-existent in this data.

The striking feature of Figure 2 is the large variability in the counting rates, i.e. the many features observed, particularly during the north polar pass. In general, the higher energy helium data follows the features in the ML counting rate except that the helium falls off more slowly, as the edge of the LPL is approached, than the protons. Although the interplanetary intensities increased with time (c.f. Fig. 1), the maximum and minimum rates in the plateau regions of the north and, about thirty minutes later, the south profiles are comparable. Thus most of the structure can be attributed to prompt or delayed access of interplanetary ions to various impact zones within the polar caps. The differences between north and south structures were due to the more favorable connection of IMF field lines from the Sun to the southern polar cap and magnetotail field lines. (The interplanetary magnetic field, as measured by IMP-8 and obtained from NSSDC's OMNI dataset, was directed about 20° northward of the Ecliptic and at about 310° to the earth-sun line in Geocentric Solar Ecliptic coordinates.) The broad high intensity plateau for the more energetic helium ions in the HPL on the dayside of the south polar cap marks direct ion access through the dayside magnetopause from the IMF. In contrast the nightside northern cap showed a broad region of minimum rates indicating poorly connected access, probably via entry points in the distant magnetotail.

The relative comparison of rate structures for protons and higher rigidity helium ions provides information on the permeability and the level of wave-particle turbulence at entry sites along the magnetopause, and on the proximity to one another of the proton and helium access points. Morfill and Quenby (1971) have noted that protons below a few MeV in energy would be scattered and isotropized by Kelvin-Helmholtz instabilities at the magnetopause. When the maximum helium rates in the HPL region are normalized to those for protons, as in Figure 2, helium shows relatively higher normalized counting rates in the LPL regions at the edges of the polar plateau, extending equatorward towards the cutoff. The helium enhancement becomes particularly large in the LPL region adjacent to the dayside magnetopause where the greatest degree of turbulence (and resultant effects on low energy protons) would be expected. Regions showing more similar intensity structures for protons and helium would then, more likely, have access through common entry points at more quiescent magnetopause locations on the flanks of the magnetosphere and in the distant magnetotail.

Turning next to the pitch angle distributions shown in Figure 2, there is little correlation to the large intensity changes marking transitions between points having prompt, delayed, or attenuated access. The mean pitch angle is relatively constant over the north polar pass and shows a slight increase during the south polar pass from the dayside to the nightside. The alignment and finite aperture of the telescope with respect to local polar field lines precluded sensitivity to trapped or quasi-trapped ions peaking in intensity at large pitch angles. In fact, the measured pitch angle distributions, plotted in Figure 3 for average, high, and low particle intensities, showed no sign of quasi-trapping and instead had higher intensities at lower pitch angles, leveling off to broad maxima for pitch angles $\geq 20°$. (These distributions were calculated using response functions dependent on particle energy and incidence angle.) The observed falloffs in the distributions towards larger pitch angles are probably not artifacts of the Main Telescope's angular response. Thus, the data indicate a particle population (helium) that is generally "field-aligned" over most of the polar cap.

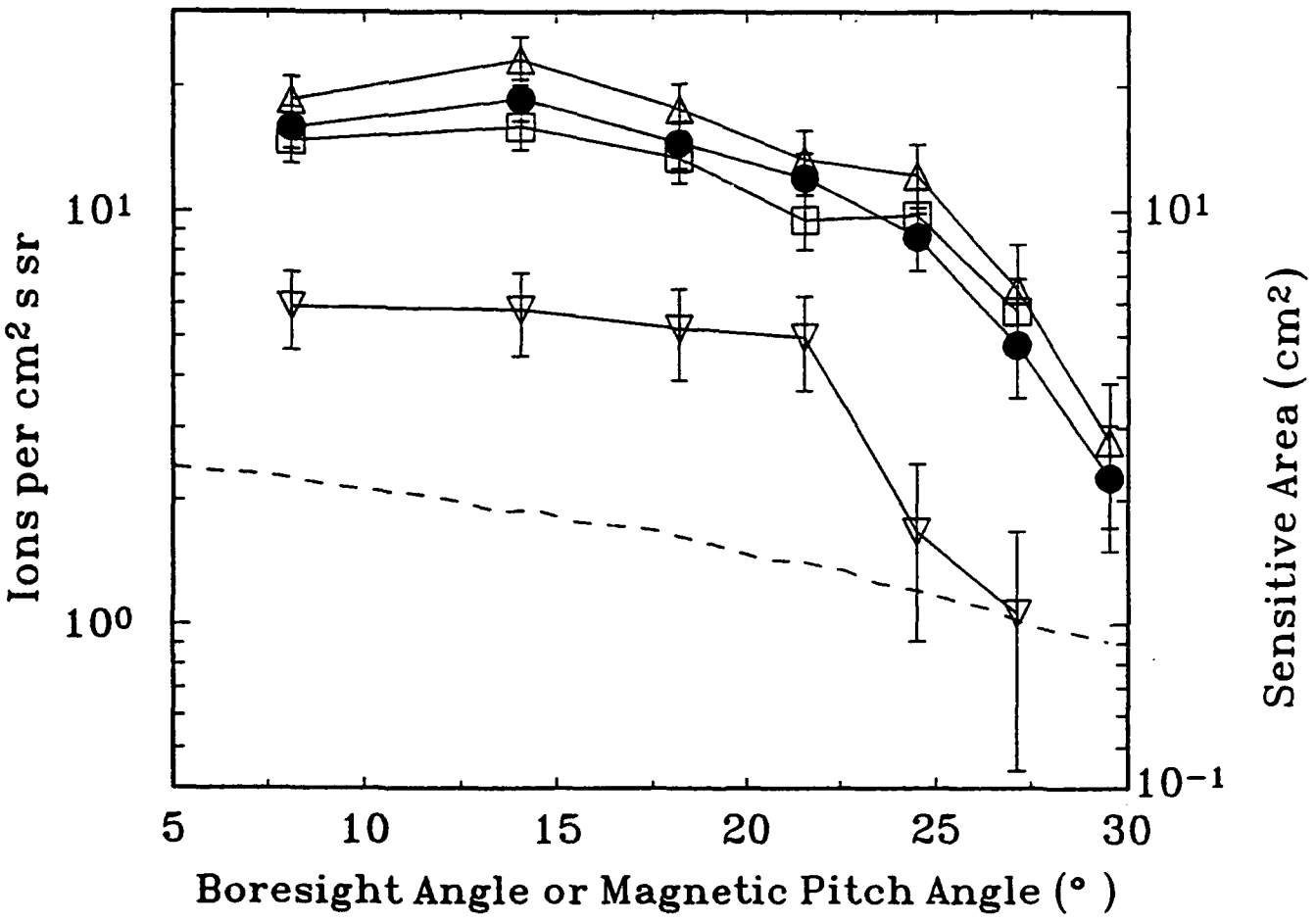

Figure 3. Directional intensities versus local pitch angle for helium ions (P3 events) measured at average (●), high (P3 > 2.5 cps: Δ), and low (P3 ≤ 2.5 cps: ▽) counting rates during the north polar crossings of orbit 1171 and at average rates (□) across the south polar cap. Also shown is the sensitive area of the ONR-602 main telescope versus angle to the boresight axis (dashed curve).

Within the HPL region these "field aligned" distributions indicated that the ions were following field lines connecting from entry points at least 100 R_E down the magnetotail from Earth, as has been predicted for low energy protons propagating near the neutral sheet. Lack of pitch angle changes across the boundaries from the HPL to the LPL indicates that the observed LPL ions were also entering the magnetosphere on tail-like field lines, or, perhaps, on dayside field lines connecting directly to the IMF. In either case, the absence of large loss cones in the center of our instrument's field of view indicates a corresponding absence of quasi-trapped ions during the period of observation.

What remains to be done is to use direct measurements of interplanetary ions (e.g., IMP-8) to predict spatial gradients and anisotropies along the magnetopause from near Earth to the deep tail region. Then magnetospheric particle tracing codes could be used to map penetrating ion distributions to the polar cap regions for comparison with the observed polar cap intensity profiles. Parameters in magnetospheric field models used by the tracing codes could then be tested by the degree of agreement between predicted and observed polar cap profiles. This is a large program which will be undertaken as time and resources permit.

III. The CRRES Environment

In order to determine the effects of the near-Earth space environment on spacecraft components, and in particular to compare to the results of the Micro-electronics Package (MEP) on CRRES, it is necessary to determine the Linear Energy Transfer (LET) spectrum of the incident radiation field. Since the electronic parts are typically covered by some amount of material, it is necessary to perform the LET calculations for a variety of shielding thicknesses. The calculation itself is relatively straight-forward once the flux and energy spectra of all of the individual elements in the radiation are known.

For the high LET region, it is the heavy ions in the cosmic rays and among SEP that are most important. Since ONR-604 was selected for the CRRES mission, in part because it could provide measurements of the heavy ion component, we have devoted some of our effort to providing this input spectra for LET calculations. In particular, we have developed the first version of a heavy ion model, considering both galactic cosmic rays (GCR) and solar energetic particles as separate particle populations.

For the GCR, the spectra outside the heliosphere in local interstellar space (LIS) are expected to be constant over very long time periods, but in the vicinity of Earth the cosmic ray intensity at energies less than ~5 GeV/nucleon can vary dramatically according to the level of solar activity. The GCR model makes use of this fact and consists, simply, of a LIS database input to a program that calculates the effects of solar modulation. Once the LIS database is determined, using a full calculation of cosmic ray interstellar transport and requiring a fit to available measurements, the near-Earth GCR spectra for a given time period can be derived by adjusting, in essence, a single parameter representing the appropriate level of modulation. Such a model is founded upon our current understanding of cosmic rays and assures agreement with the spectral measurements. The energy spectra resulting from the model covers the energy range 50-50,000 MeV/nucleon for each isotope from ^{1}H to ^{58}Ni.

For SEP's, a model must be based upon individual events since there is considerable variability from one SEP event to the next. There are five steps in modeling a SEP event:
(1) Determine the time-intensity profile including the start, peak and end of the SEP event.
(2) Obtain peak and average fluxes for helium and protons and fit each to a power-law form:

$$dJ/dE = A(E/E_0)^{-\gamma},$$

where E_0 is a "representative energy" for each SEP event. (The Helium spectral index γ is then assumed to be the spectral index for all the heavy elements.) (3) Calculate the integrated fluence F (in particle/cm^2-sr-MeV/nucleon). (4) Find the heavy-ion enrichment parameter α, which is defined by Chenette and Dietrich (1984) as $\alpha = (\ln Fe/O - \ln 0.045)/18$, where 0.045 is the typical solar system value for the *Fe/O* abundance ratio. (5) Apply the α parameter to scale the solar energetic heavy-ion fluxes of different heavy ion species from the solar helium spectrum. This yields inferred spectra for all of the heavy elements, from which the LET spectra can be calculated for various thicknesses of shielding. In addition, it is necessary to determine the proton spectrum for each event in order to fill in the low LET region.

During this quarter, some of our effort has been devoted to finalizing the results from these initial models, and preparing manuscripts. The initial results were presented at the COSPAR meeting, part of the World Space Congress held in Washington, DC. Our rough manuscripts were selected by the section organizers for inclusion as papers in Advances in Space Research. Each manuscript was submitted to a reviewer, and the reviewer's comments and suggestions were then incorporated into the final manuscripts which were submitted to the editors for publication sometime in 1993. Copies of these papers follow.

CONTRIBUTIONS TO

THE WORLD SPACE CONGRESS,

COMMITTEE ON SPACE RESEARCH (COSPAR),

And papers prepared/accepted for publication in

Advances in Space Research

(1) "Cosmic Ray Heavy Ion Penetration Deep Into the Magnetosphere: Results from S81-1 and CRRES," J.F. Cooper, J. Chen, T.G. Guzik, Y. Sang and J. P. Wefel.

(2) "A Model of Galactic Cosmic Rays for Use in Calculating Linear Transfer Spectra," J. Chen, D. Chenette, R. Clark, M. Garcia-Munoz, T.G. Guzik, K.R. Pyle, Y. Sang, and J.P. Wefel.

(3) "A Model of Solar Energetic Particles for Use in Calculating LET Spectra Developed from ONR-604 Data," J. Chen, D. Chenette, T.G. Guzik, M. Garcia-Munoz, K.R. Pyle, T. Sang and J.P.Wefel.

(4) "The LET Spectrum and Its Uncertainty During the CRRES Mission," D.L. Chenette, T.G. Guzik and J.P. Wefel.

COSMIC RAY HEAVY ION PENETRATION DEEP INTO THE MAGNETOSPHERE: RESULTS FROM S81-1 AND CRRES

J. F. Cooper*, J. Chen**, T. G. Guzik**, Y. Sang** and J. P. Wefel**

*National Space Science Data Center/Hughes STX Corporation, Code 633, NASA Goddard Space Flight Center, Greenbelt, MD 20771, U.S.A. **Department of Physics and Astronomy, Louisiana State University, Baton Rouge, Louisiana 70803-4001, U.S.A.

ABSTRACT

In spite of strong magnetic shielding by the geomagnetic field, small fractions (1-10%) of the total high energy, heavy ion intensities of solar and galactic cosmic rays have been observed at energies below theoretical cutoffs for direct entry into the earth's magnetosphere from interplanetary space. We report on measurements of these heavy ions at 10 to 500 MeV/nucleon by cosmic ray composition experiments on the *S81-1* satellite in polar orbit during 1982 and on the *CRRES* satellite in geosynchronous transfer orbit during 1990-1991.

INTRODUCTION

The heavy ion components of the solar and galactic cosmic rays are of considerable interest for cosmic ray experiments conducted within the geomagnetic field, because atomic charge states may in principle be determined from comparison of measured ion energies to calculated magnetic cutoffs for direct penetration from outside the magnetosphere. The expected Q = +1 effective charge of the anomalous component of cosmic ray ions was confirmed during the 1984-1988 solar minimum with this method by a series of experiments on *Cosmos* satellites in high inclination orbits at altitudes of 250 to 400 km /1/ and by *Spacelab 1* /2/ and *Spacelab 3* /3/ experiments onboard the NASA Space Shuttle. The Cosmos data analysis relied on geomagnetic modeling of orbital intensity averages, while the *Spacelab* experiments allowed detailed analysis of individual but far fewer events. Whereas the anomalous component dominates the galactic cosmic rays only below 50 MeV/nucleon and only near solar minimum, the *Spacelab 3* experiment found evidence in 1985 for partially ionized ($1 < Q < Z$) heavy nuclei above neon at energies of 30 - 100 MeV/nucleon /4/. In contrast the solar energetic ions measured near 10 MeV by the *Cosmos* experiment series were found to be almost fully ionized (Q = +7 for oxygen) and consistent with direct charge state measurements at lower energies /5/.

S81-1 & *CRRES* EXPERIMENTS

The *S81-1* and *CRRES* (Combined Release and Radiation Effects Satellite) satellites were launched by the U.S. Air Force Space Test Program and carried science experiments designed to investigate the energetic particle environment of the earth's magnetosphere and its potential effects on satellite microelectronics. *S81-1* went into a sun synchronous (10:30 AM/PM local time) polar orbit at an altitude range of 180 - 270 km and had a gravity-gradient orientation such that the University of Chicago cosmic ray experiment, designated as ONR-602 /6/, pointed upwards towards zenith at all times and viewed ions precipitating into the atmosphere. *CRRES* carried the Chicago ONR-604 /7/ cosmic ray instrument and other experiments in a geosynchronous transfer orbit (GTO) with perigee 350 km, apogee 33,600 km, an inclination of 18 degrees, and an orbital period of ten hours. The two rpm spin rotation of *CRRES*, and the wide acceptance angle (±40 deg.) of the ONR-604 main telescope, allowed measurements over a wide range of ion arrival directions. Both missions operated during periods near solar maximum of low to high solar flare activity: 28 May to 5 December 1982 for *S81-1* and 25 July 1990 through 12 October 1991 for *CRRES*.

The ONR-602 and ONR-604 instruments both used solid state detectors for high resolution measurements of ion energy, isotopic nuclear mass, and nuclear charge. Ion incidence trajectories were determined within a few degrees by utilization of solid-state position sensing detectors for calculations of energy loss pathlengths within single detectors and of angular distributions. The *S81-1* instrument was designed to measure 4 - 230 MeV/nucleon ions from helium through iron, while the *CRRES* instrument was configured for measurements of the galactic cosmic ray ions at 25-500 MeV/nucleon for protons through iron and had additional shielding for the GTO orbit environment.

GEOMAGNETIC ANALYSIS OF ATOMIC CHARGE STATES

In this report we focus on the relative distributions of solar and galactic cosmic ray ions, in particular the heavy ions from carbon through iron with minimal magnetospheric background, which were detected at energies above and below theoretical energy cutoffs computed from geomagnetic field models. Our approach was most comparable to the individual event analysis of the *Spacelab* experiments /2,3/, since the times and geomagnetic locations of individual events were fully resolved. Since we could not distinquish a directly penetrating ion from a trapped or quasi-trapped one, all analysed ions were assumed to be penetrating. If a fully stripped ion nucleus of charge Z could reach the spacecraft at the detection point within the magnetosphere, we calculated a maximum atomic charge $Q < Z$ that would allow the direct entry. With the measured ion parameters, also including energy and incidence trajectory, a standard numerical code was used to trace the ions backwards in time along the arrival trajectory until (1) an arbitrary boundary at 25 earth radii was reached (i.e., indicating an allowed direct entry trajectory), (2), the ion entered the earth's atmosphere, or (3) the calculation terminated after a fixed number of steps within the magnetosphere and indicated a trapped or quasi-trapped ion trajectory. In cases (2) and (3) successive calculations were done with lower Q values until a direct entry trajectory was found. In general we used the Z - Q parameter (i.e., the number of atomic electrons) to separate events with energies above or below local cutoffs for direct entry. The numerical code used the IGRF 1980 internal field model and the Tsyganenko 1987 /8/ external field model to calculate magnetic fields along the ion trajectories. Since these models were derived from empirical fits to time averaged field data, significant variations from the model fields were expected for the actual fields. Effects of large geomagnetic disturbances were minimized by selecting only data for intervals when $Kp \leq 5$. Even so, uncertainties of order unity in Z - Q should be assigned to our charge state calculations.

OBSERVATIONS

During the *S81-1* mission ONR-602 responded mostly to flare ions below 50 to 80 MeV/nucleon for the several large flares in 1982, notably the series of flares during 3-6 June, 9-13 July 9-13, and 22-26 November. The highest intensities were recorded on 13-14 July. Despite the relatively low level of flare activity during days 210 to 320 of 1982 there was a steady sprinkling of ions at 50-200 MeV/nucleon of non-solar origin, most probably galactic cosmic rays. ONR-604 also operated during an active period, including large flares in March and June of 1991, but the higher energy response of ONR-604 to heavy ions at 80-500 MeV/nucleon was largely due to non-solar cosmic ray sources and the measured intensities were relatively uniform in time as compared to the ONR-602 events.

Percentages of events with energies significantly below cutoff, possibly due to partial ionization ($Z - Q > 1$), were about ten percent (214 out of 1770 events) for the *S81-1* events and less than one percent (38 out of 5004) from the *CRRES* events. Most of the *S81-1* events with calculated low charge states ($Z - Q > 0$) were from large flares, despite the removal of high Kp events, rather than from the higher energy galactic component. The fewer *CRRES* events, and those at higher energies from *S81-1*, were widely dispersed over the mission as expected for galactic cosmic rays.

The spatial distributions in L of events from each mission are shown in Figure 1 (a), where the lower altitude penetrations of the *CRRES* events for $Z - Q > 1$ were consistent with the higher energies of these events. The greater number of *S81-1* events was, however, most likely due to the differences in the *S81-1* and *CRRES* orbits, the latter being highly elliptical with peak instrument livetimes near apogee and minimal livetimes at lower altitudes. In Figure 1 (b) the relative abundances of ions over the range of calculated Q values are shown for oxygen, the most abundant element measured by either experiment. All the $Z - Q > 0$ oxygen events from *S81-1* were well separated in abundance from the large $Q = Z$ peak, but there was significant spill over into the $Q = 7$ bin from the main *CRRES* event peak. This difference in charge separation was most likely due to greater time variation of the actual magnetic field at higher L values along the GTO orbit of *CRRES* in comparison to the stable internal field

which dominated along the lower-altitude *S81-1* orbit. It is worth noting that both the *S81-1* and *CRRES* oxygen charge distributions were both consistent with the average atomic charge being equal to Z, while the relatively few but still identifiable Z - Q > 0 events might have had different origins from the fully stripped ions.

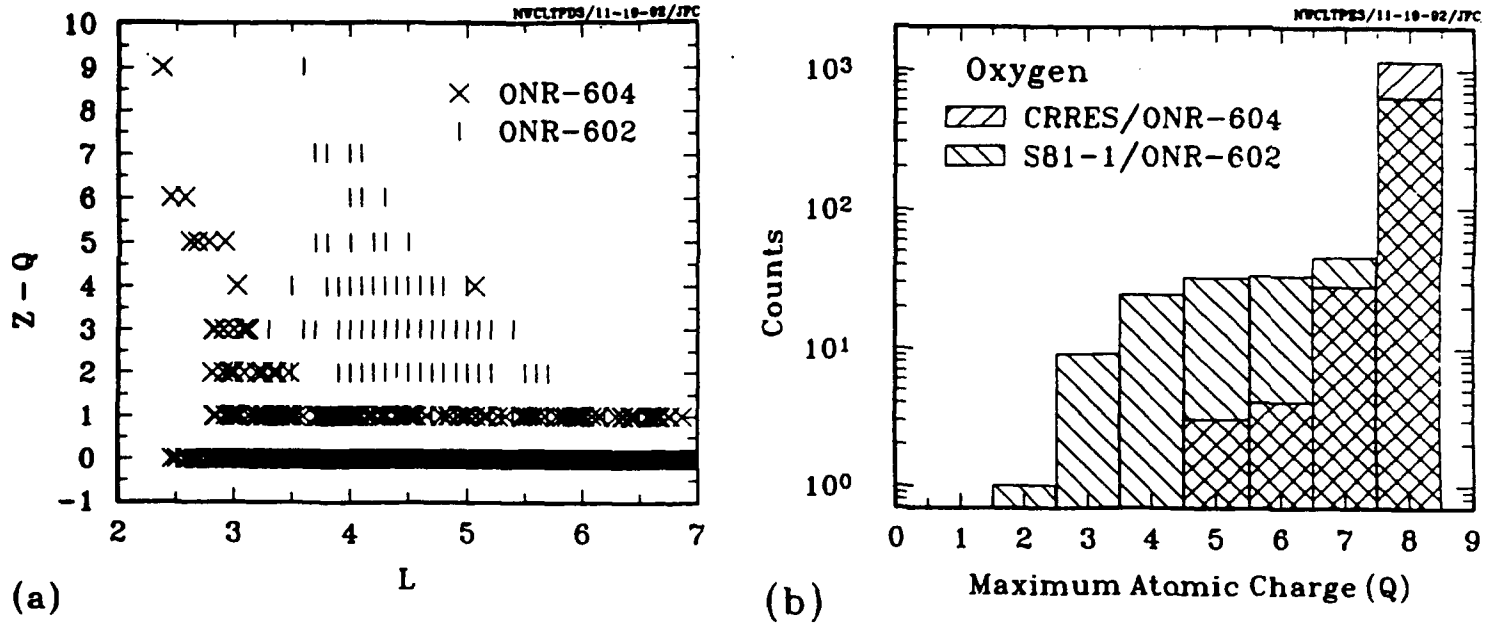

Fig. 1. (a) Correlation of calculated Z - Q values vs. magnetic L value for both experiments; (b) Histograms of calculated maximum atomic charge (Q) values for oxygen (Z=8) events from both experiments.

The total and Z - Q > 1 abundances of the measured elements from carbon through the iron group are compared in Figure 2 (a) and (b) with solar system values (Cameron-1982 /9/) normalized to the observed total abundance of silicon (Z=14) in each case. In Figure 2 (a) only the more abundant charge peaks are shown, based on a recent recalculation of the measured element assignments, and the relative abundances were roughly in agreement with the solar system values as expected for solar energetic ions. Within statistical errors the partially ionized events also followed the solar abundances, except that the two iron events appeared underabundant relative to the seven to nine measured events for even-Z peaks in the neon-silicon range. However, these raw abundances lack spectral corrections which would have given higher relative iron group abundance at the same energy/nucleon, particularly for the relatively steeper energy spectra of the solar energetic ions as compared to the harder galactic ion spectra. In the higher energy range the total elemental abundances of the *CRRES* events in Figure 2 (b) showed significant enhancements of odd-Z and sub-iron (Z=21-25) nuclei which were characteristic of galactic cosmic ray propagation through diffuse matter in the interstellar medium. Among the few partially ionized events there were also relatively many odd-Z ions, perhaps indicating commonality of origin with the galactic ions and their interstellar propagation.

CONCLUSIONS

Partially ionized fractions of solar and galactic heavy ions were small but measurable during two solar maximum periods, 1982 and 1990-1991, when the singly charged anomalous component of cosmic ray ions was not observed. The solar ions were distinctly resolved at Z - Q > 0 with the expected solar composition as a ten percent fraction of the observed flare ion population, while partial ionization states constituted less than one percent of the total galactic ion intensity measured by *CRRES*. We cannot rule out the possibility that secondary heavy nuclei from nuclear interactions in the earth's atmosphere, rather than in the interstellar medium, provided the bulk of our Z - Q > 0 event sample for quiet-time measurements of ions near and above 100 MeV/nucleon. Increased statistics from the ongoing *SAMPEX* (launched in 1992) and forthcoming *NOAA-I*/EHIC (launch planned in 1993) cosmic ray experiments in polar orbits are required for definitive composition and charge state analyses and for investigation of cosmic ray sources and effects of solar modulation over solar cycle time scales. Position sensing detectors in the SAMPEX and EHIC experiments, the main telescope of the latter being nearly identical to that of ONR-602, will support composition measurements at high isotopic resolution and angular measurements of local arrival directions at the respective spacecraft, the latter being useful for particle tracing and rigidity cutoff calculations.

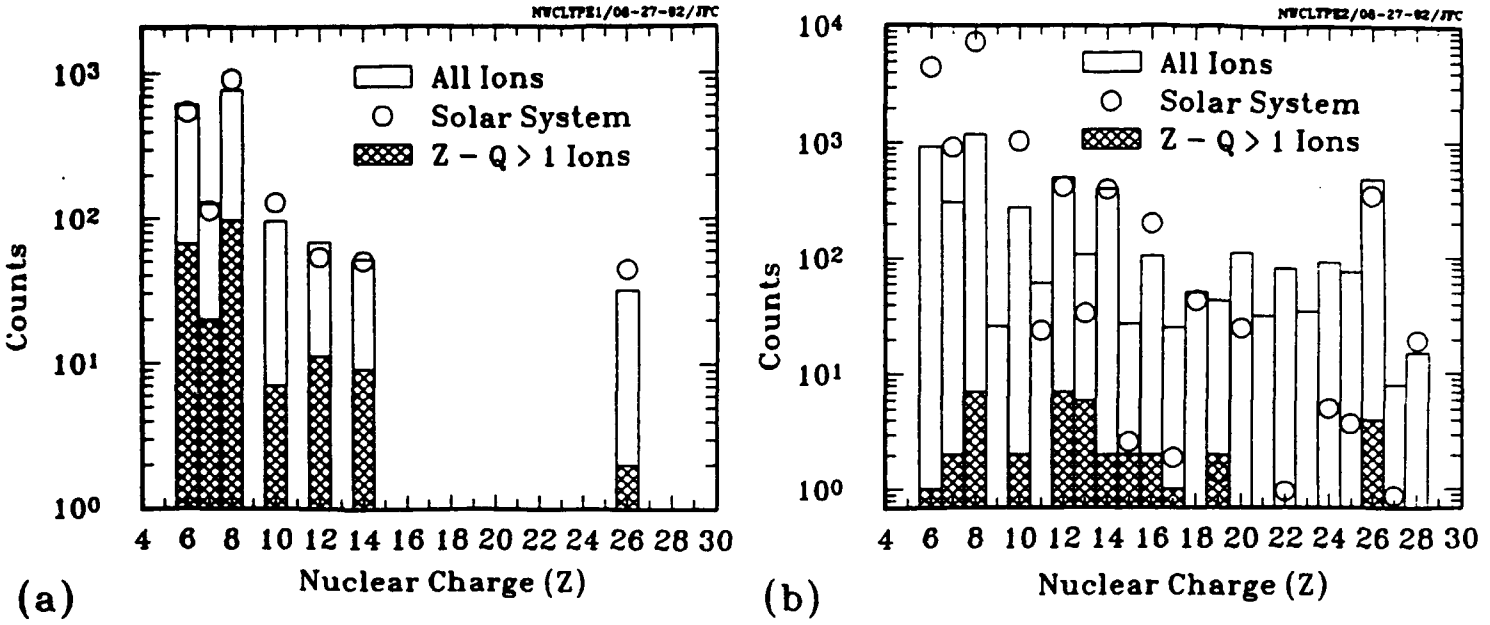

Fig. 2. Solar system Z abundances (normalized to Si) relative to observed values from (a) *S81-1* and (b) *CRRES*.

ACKNOWLEDGEMENTS

Data analysis and geomagnetic modeling for this work were supported at the National Space Science Data Center by NASA through Hughes STX Corporation and at Louisiana State University by U.S. Air Force Contract F19628-90-K-0026 and Office of Naval Research Grant N-00014-90-J-1466. The ONR-602 and ONR-604 experiments were developed by the group of Professor John A. Simpson, Principal Investigator for both experiments, at the University of Chicago under NASA Contract NAS 2-24430. Both experiments were sponsored for flight by ONR with launch support and telemetry coverage provided by the U. S. Air Force Space Test Program.

REFERENCES

1. J. H. Adams, Jr., M. Garcia-Munoz, N. L. Grigorov, B. Klecker, M. A. Kondratyeva, G. M. Mason, R. E. McGuire, R. A. Mewaldt, M. I. Panasyuk, CH. A. Tretyakova, A. J. Tylka, and D. A. Zhuravlev, *Astrophys. J. (Letters), 375*, L45 (1991).

2. K. Oschlies, R. Beaujean, and W. Enge, *Astrophys. J. 345*, 776 (1989).

3. R. K. Singh, B. Mitra, N. Durgaprasad, S. Biswas, M. H. Vahia, J. S. Yadav, A. Dutta, and J. N. Goswami, *Astrophys. J., 374*, 753 (1991).

4. S. Biswas, N. Durgaprasad, B. Mitra, R. K. Singh, A. Dutta, and J. N. Goswami, *Astrophys. J. Lett., 359*, L5 (1990).

5. A. Luhn, B. Klecker, D. Hovestadt, G. Gloeckler, F. M. Ipavich, M. Scholer, C. Y. Fan, and L. A. Fisk, *Adv. Sp. Res., 4*, 161 (1984).

6. J. A. Simpson, J. P. Wefel, and R. Zamow, *Proc. 18th International Cosmic Ray Conf., Bangalore, 10*, 322 (1983).

7. M. Garcia-Munoz, K. R. Pyle, and J. A. Simpson, this issue.

8. N. A. Tsyganenko, *Plan. Sp. Sci., 35*, 1347 (1987).

9. A. G. W. Cameron, in: *Essays in Nuclear Physics*, Cambridge Univ., Cambridge 1982, p. 23.

A MODEL OF GALACTIC COSMIC RAYS FOR USE IN CALCULATING LINEAR ENERGY TRANSFER SPECTRA

J. Chen[2], D. Chenette[1], R. Clark[2], M. Garcia-Munoz[3], T. G. Guzik[2], K. R. Pyle[3], Y. Sang[2], and J. P. Wefel[2]

[1]Lockheed Palo Alto Research Lab., 3251 Hanover Street, Palo Alto, CA 94304, USA; [2]Department of Physics and Astronomy, Louisiana State University, Baton Rouge, LA 70803, USA; [3]Enrico Fermi Institute, University of Chicago, 933 E. 56th Street, Chicago, IL 60637, USA

ABSTRACT

The galactic cosmic rays (GCR) contain fully stripped nuclei, from Hydrogen to beyond the Iron group, accelerated to high energies and are a major component of the background radiation encountered by satellites and interplanetary spacecraft. This paper presents a GCR model which is based upon our current understanding of the astrophysics of GCR transport through interstellar and interplanetary space. The model can be used to predict the energy spectra for all stable and long-lived radioactive species from H to Ni over an energy range from 50 to 50,000 MeV/nucleon as a function of a single parameter, the solar modulation level ϕ. The details of this model are summarized, ϕ is derived for the period 1974 to present, and results from this model during the 1990/1991 CRRES mission are presented.

INTRODUCTION

CRRES (Combined Release and Radiation Effects Satellite) was launched on July 25, 1990, in part, to study and characterize the effects of energetic charged particles incident upon electronic devices. As charged particles pass through or stop within the sensitive volume of a microelectronic circuit a large amount of ionization may be produced, simulating a logic state change and causing a single event upset (SEU). In principle, the SEU rate for a particular chip geometry can be calculated if the linear energy transfer (LET) spectra (a convolution of the particle environment composition, energy spectrum and stopping power) is first determined. The CRRES mission carried a Microelectronics Package (MEP) to measure the SEU phenomenon for a variety of chips and an additional series of instruments which were used to characterize the in-situ energetic particle environment.

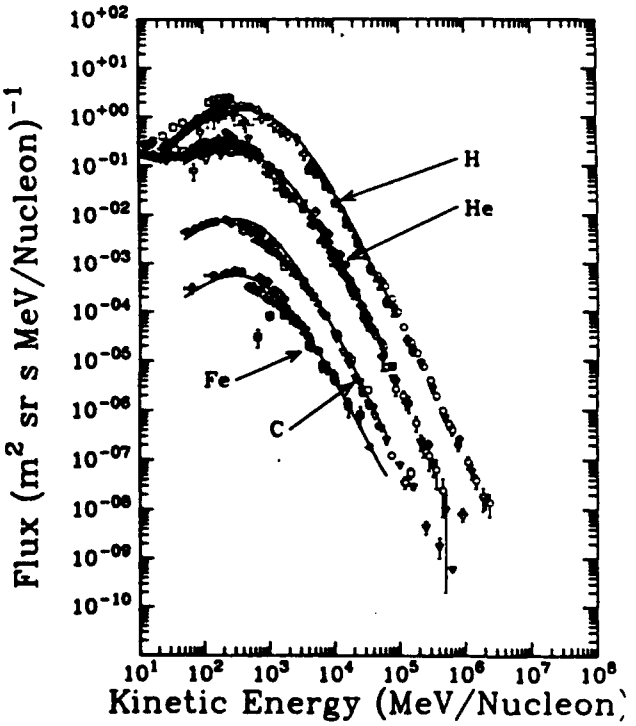

Fig. 1. Energy spectra measurements and model predictions for H, He, C and Fe.

One such instrument, ONR-604, was designed to measure high energy, heavy ions covering the charge range $1 \leq Z \leq 28$ and the energy range 40 - 100 MeV/nucleon for Helium up to 180 - 500 MeV/nucleon for Iron. The abundance of heavy ions in a particle population can be only a fraction of H or He, but ionization energy is deposited in proportion to charge squared and, hence, the high charge species constitute an important component of the LET spectra. To properly determine the LET, full energy spectra for all isotopes are needed, however, an instrument such as ONR-604 will deliver, for short integration time periods (< 6 months), a spectrum segment for the most abundant species. Thus, a model must be used to fill in the gaps, matching the available data and providing energy spectra over energy and charge regions not covered by the measurements.

The energetic (>50 MeV/nucleon) heavy ion particle population in the vicinity of Earth is generally dominated by two principal components; the Solar Energetic Particles (SEP) which are associated with solar flare eruptions and the Galactic Cosmic Rays (GCR) which originate outside the heliosphere. This paper describes a GCR model which is based upon our current understanding of cosmic ray astrophysics. Companion papers at this conference describe a SEP Model /1/ and application of the SEP / GCR model results to calculations of the LET spectrum for the CRRES mission /2/.

THE GCR MODEL

The GCR spectra outside the heliosphere in local interstellar space (LIS) are expected to be constant over very long time periods, but in the vicinity of Earth the cosmic ray intensity at energies less than ~5 GeV/nucleon can vary dramatically according to the level of solar activity. The GCR model makes use of this fact and consists, simply, of a LIS database input to a program that calculates the effects of solar modulation. Once the LIS database is determined, using a full calculation of cosmic ray interstellar transport and requiring a fit to available measurements, the near-Earth GCR spectra for a given time period can be derived by adjusting, in essence, a single parameter representing the appropriate level of modulation. Such a model is founded upon our current understanding of cosmic rays and assures compliance with the particle measurements. The energy spectra resulting from the model covers the energy range 50 - 50,000 MeV/nucleon for each isotope from H to Ni contained in the galactic cosmic ray population and can be directly used to compute the LET spectrum as a function of time /2/.

Determining the GCR Local Interstellar Spectrum

Over the years a wealth of data on cosmic ray spectra near the orbit of Earth has been collected as illustrated in Figure 1 which shows available data for a selected set of elements. Much of the lower energy data (i.e. < 1 GeV/nucleon) in the figure was obtained during an extended period of minimum solar modulation conditions (~1975 - 1978) when the cosmic ray flux was at a maximum. Similar measurements are available for almost every element in the cosmic rays, with varying accuracy and energy coverage. These are the primary data used to provide multiple constraints when deriving the GCR local interstellar spectra. In addition, elemental ratio measurements augment the spectra data, and isotopic ratio measurements are also available. The most accurate isotope results are for elements with charge less than Sulfur at energies less than ~600 MeV/nucleon.

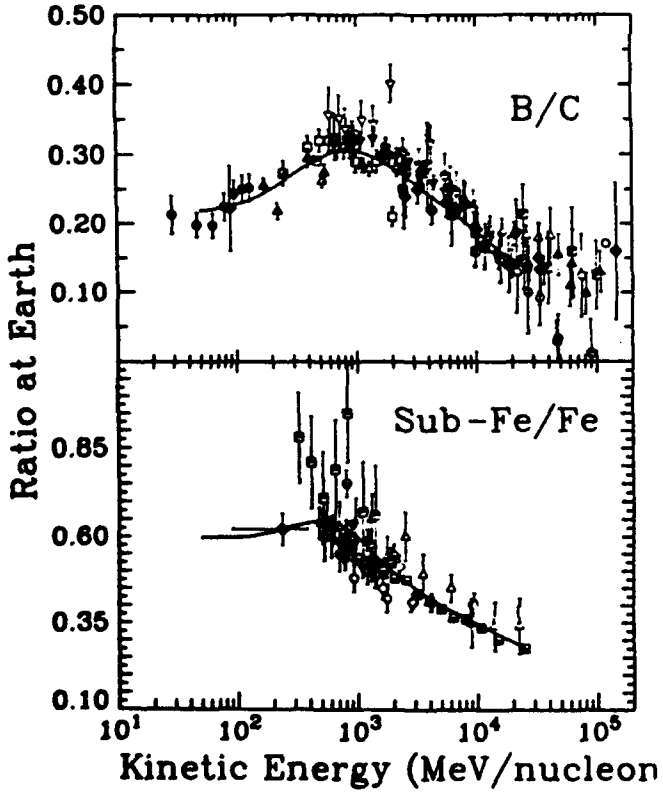

Fig. 2. Secondary/Primary ratio measurements and model predictions.

The curves in Figure 1 show the GCR model predictions using a solar modulation level appropriate to solar minimum. The LIS were calculated with a numerical simulation of cosmic ray transport through interstellar space with the GCR source and propagation characteristics adjusted until a good fit to the measurements were obtained. The numerical simulation is based upon the weighted-slab propagation technique /3/ and is described by Garcia-Munoz et al. /4/. This technique involves calculating the effects of ionization energy loss, radioactive decay, electron pickup and loss, and nuclear interaction fragmentation loss, production and kinematics for a series of thin slabs of interstellar matter. The slab results are then integrated over a pathlength distribution (PLD) which can be related to particular astrophysical models /5/. In practice, the PLD is usually determined empirically by fitting ratios of secondaries (little or no abundance at the cosmic ray source) to primaries (present at the source). Secondary components are produced entirely from the fragmentation of primary species and are particularly sensitive to details of cosmic ray transport. Such ratios include B/C and (Sc+Ti+V+Cr+Mn)/Fe as shown in Figure 2 along with the predictions of the GCR model.

Determining the Solar Modulation Level

With the baseline LIS determined, the effects of solar modulation must be calculated for each time period of interest. The program used for this calculation is a spherically symmetric model of the heliosphere that includes the effects of diffusion, convection and adiabatic deceleration /6/ and has been used successfully to model the modulation of electrons, protons and heavier nuclei over several solar cycles /7,8/. The level of modulation at a heliospheric radius r is given by the parameter

$$\phi(r) = \frac{1}{3}\int_r^R \frac{V(r')}{K(r')}dr' \qquad (1)$$

where V(r') is the solar wind velocity, K(r') is the radial part of the diffusion coefficient and R is the radius of the heliosphere. It is this single parameter,which specifies the modulation intensity and values of R, r, V and K yielding the same value of ϕ will result in similar modulated spectra /9/.

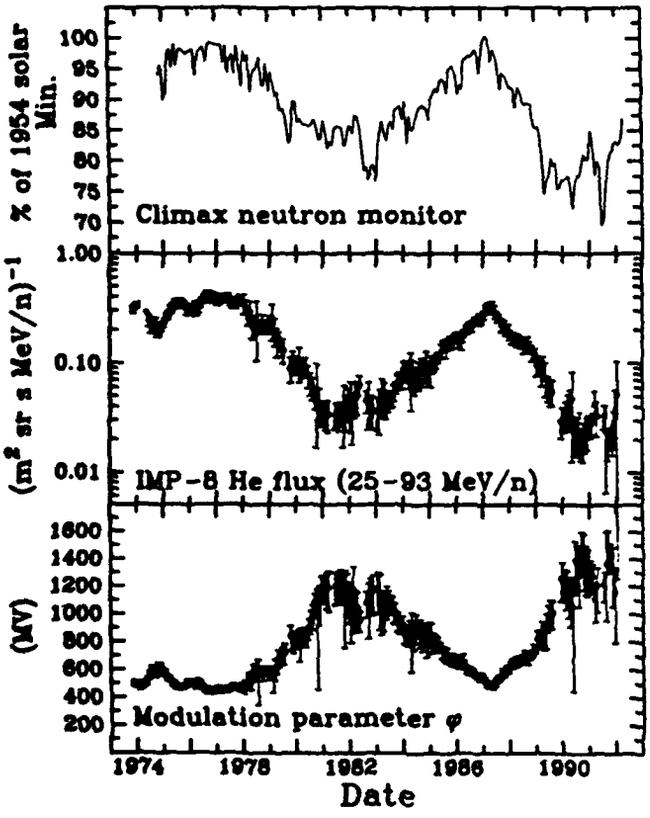

Fig. 3. The solar variations from 1973 to present for the Climax neutron monitor (top), the IMP-8 25-93 MeV/nucleon Helium flux (middle), and the solar modulation level (bottom).

For this GCR model, ϕ is determined from a portion of the Helium spectrum measured by the IMP-8 interplanetary spacecraft. Monthly averages, cleaned of solar flare periods and anomalous rate spikes, are shown in the middle panel of Figure 3. These data track the solar cycle with maximum flux values during solar minima (~1975-1979 and ~1987-1988) and a minimum flux level during solar maxima (~1980-1983 and ~1990-1992). The error bars show the variance of the He flux over the time period, and these fluctuations are largest for solar maximum conditions. Further, periods of low solar activity ("quiet time") are not frequent during solar maximum, resulting in occasional gaps in the time coverage. The top panel of Figure 3 shows results from a Univ. of Chicago ground based neutron monitor located at Climax, Colorado over the same time period. The neutron monitor is sensitive to the high energy (>3 GV) cosmic ray flux at Earth, and there is a clear correlation with the lower energy interplanetary Helium flux.

The bottom panel of Figure 3 shows the derived value of ϕ using a method similar to that of Garcia-Munoz et al. /8/. The Helium LIS is fixed, and ϕ is adjusted until the calculated spectrum matches the flux measurements. We have compared the results of Figure 3 with previous work /4,7/ that determined ϕ over the time period 1974 - 1980 and the results are in good agreement. As an additional cross check we also determined ϕ from Oxygen spectra measured by IMP-8 over a time period (8/90 to 3/91) during the recent solar maximum. A chi-squared minimization fit to these data yield ϕ = 1444 ± 42 MV which is consistent with ϕ = 1330 ± 110 MV derived from the Helium measurements. In later releases of this model we expect to use ONR-604 flux measurements to refine the level of modulation determined here.

MODEL RESULTS FOR CRRES

Figure 4 shows GCR model results for 1990 and 1991. The CRRES operational lifetime from its launch on 25 July 1990 till an unrecoverable systems failure on 12 October 1991 is shown as the horizontal line on the bottom panel of Figure 4. Throughout this period ONR-604 on-board CRRES performed well and the data analysis is well underway. The top panel of Figure 4 presents the Helium count rate derived from the ONR-604 pulse height analysis P2 rate for "quiet times" and for L > 6. When these data are compared with the IMP-8 Helium measurements (bottom panel, filled circles) the same relative trend is evident, indicating a good correlation between the interplanetary measurements and the ONR-604 results within the magnetosphere.

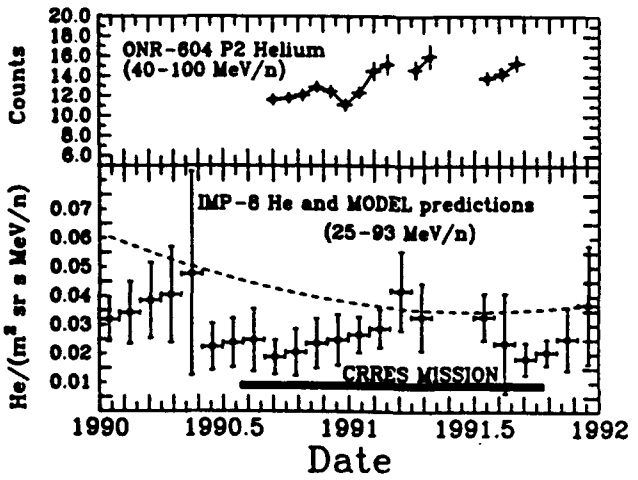

Fig. 4. The top panel shows the ONR-604 P2 Helium count rate during the CRRES mission and the bottom panel shows the IMP-8 Helium flux compared with the CREME model predictions (dashed curve).

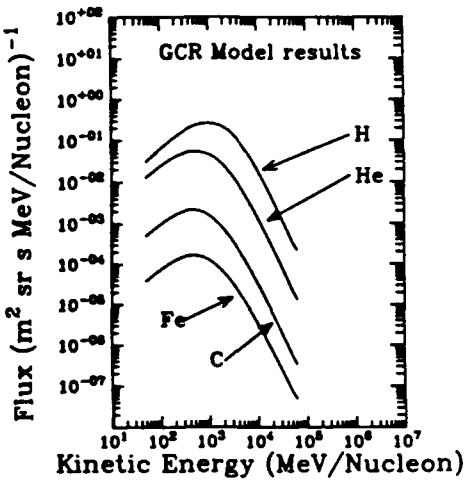

Fig. 5. The GCR model energy spectra predictions for the average solar modulation conditions during the CRRES mission.

A large gap in the monthly averaged IMP-8 Helium flux during the CRRES mission is apparent in the bottom panel of Figure 4. This was a period of intense solar activity and solar energetic particles dominate the measured particle population /1/. The flux predictions of the CREME model /10/ are shown as the dashed curve. CREME (Cosmic Ray Effects on Microelectronics) was developed in the early 1980's to provide a model of the near-Earth particle environment for calculating LET and SEU rates. This particle environment is expressed by a series of analytic formula for the energy spectra and solar cycle variations. While CREME predicts a minimum He flux during the 1991 period of intense solar activity the general trend does not follow the actual measurements. Further, for the time period 8/90 to 3/91 CREME over-estimates the Helium measurement by about 60% and the IMP-8 Oxygen flux by about a factor of two. Thus, it is expected that CREME will predict enhanced LET spectra and SEU rates for the CRRES mission /2/.

The average value of ϕ during the CRRES lifetime is ≈1330 MV and a selection of GCR model energy spectra for this level is shown in Figure 5. These spectra can be compared to the data and curves of Figure 1, which are for solar minimum conditions. At 100 MeV/nucleon the two sets of curves can differ by almost an order of magnitude. For CRRES the heavy ion fluxes at low energy (~100 MeV/nucleon) are at a ~20 year low as can be seen from Figure 3. In fact, over this time period the modulation level follows a very complex curve and it is not evident how future trends can be reliably predicted. What seems clear, however, is that if accurate spectra are required then a GCR model directly tied to in-situ particle measurements, such as described here, must be used.

CONCLUSIONS

A model of the galactic cosmic rays, based upon current understanding of cosmic ray astrophysics and constrained by available measurements, has been developed to predict the energy spectra of each species over a broad energy range for any quiet-time period from 1974 to the present by adjusting a single parameter; the solar modulation level ϕ. Within the CRRES time period, this model follows interplanetary measurements of the Helium and Oxygen fluxes at 100 MeV/nucleon while the CREME model overestimates these values by 60% to a factor of two. In later versions of this model we expect to improve upon the prediction accuracy by requiring simultaneous fits to heavy ion spectra measurements from IMP-8 and ONR-604.

This research is supported by NASA contracts NAGW 2368, NAG 5-706, by NSF grant ATM-9015530, by U.S. Air Force contracts F19628-90-K-0025, -0026 and F19628-90-C-0101, and by ONR grant N00014-90-J-1466.

REFERENCES

1. J. Chen, D.L. Chenette, T.G. Guzik, M. Garcia-Munoz, K.R. Pyle, Y. Sang and J.P. Wefel, A Model of Solar Energetic Particles for Use in Calculating LET Spectra Developed from ONR-604 Data, Adv. Space Res., this issue.

2. D.L. Chenette, T.G. Guzik and J.P. Wefel, The LET Spectrum and It's Uncertainty during the CRRES Mission, Adv. Space Res., this issue.

3. V.L. Ginzburg, and S.I. Syrovatshii, *The Origin of Cosmic Rays*, trans. H.S.W. Massey, ed. D. ter Haar (New York: Maxmillan), 1964.

4. M. Garcia-Munoz, J.A. Simpson, T.G. Guzik, J.P. Wefel and S.H. Margolis, Cosmic Ray Propagation in the Galaxy and in the Heliosphere: The Path-Length Distribution at Low Energy, *Ap. J. Suppl.* 64, 269, (1987).

5. C.E. Fichtel and D.V. Reames, Cosmic-Ray Propagation, *Phys. Rev.* 175, 1564, (1968).

6. L.A. Fisk in "Solar System Plasma Physics", Vol. 1 ed. E.N. Parker, C.F. Kennel and L.J. Lanzerotti (Amsterdam: North-Holland), p.179 (1979).

7. P.A. Evenson, M. Garcia-Munoz, P. Meyer, K.R. Pyle and J.A. Simpson, A Quantitative Test of Solar Modulation Theory: The Proton Helium and Electron Spectra from 1965 thorugh 1979, *Ap. J. (Letters)* 275, L15 (1983).

8. M. Garcia-Munoz, P. Meyer, K.R. Pyle, and J.A. Simpson, The 1973-1984 Solar Modulation of Cosmic Ray Nuclei, Proc. *19th Intl. Cosmic Ray Conf.* (LaJolla) 4, 409 (1985)

9. I.H. Urch and L.J. Gleeson, Energy Losses and Modulation of Galactic Cosmic Rays, *Ap. Space Sci.* 17, 426 (1972).

10. J.H. Adams Jr., Cosmic Ray Effects on Microelectronics, Part IV, NRL Report 5901 Naval Research Laboratory, (1986).

A MODEL OF SOLAR ENERGETIC PARTICLES FOR USE IN CALCULATING LET SPECTRA DEVELOPED FROM ONR-604 DATA

J. Chen[2], D. Chenette[1], T. G. Guzik[2], M. Garcia-Munoz[3], K. R. Pyle[3], Y. Sang[2], and J. P. Wefel[2]

[1]*Lockheed Palo Alto Research Laboratory, 3251 Hanover Street, Palo Alto, CA 94304. U.S.A.* [2]*Department of Physics and Astronomy, Louisiana State University, Baton Rouge, LA 70803. U.S.A.* [3]*Enrico Fermi Institute, University of Chicago. 933 E. 56th Street, Chicago, IL 60637, U.S.A*

ABSTRACT

A model of solar energetic particles (SEP) has been developed and is applied to solar flares during the 1990/1991 CRRES mission using data measured by the University of Chicago instrument, ONR-604. The model includes the time-dependent behavior, heavy-ion content, energy spectrum and fluence, and can accurately represent the observed SEP events in the energy range between 40 to 500 MeV/nucleon. Results are presented for the March and June, 1991 flare periods.

INTRODUCTION

Ionization caused by an incident energetic particle, particularly heavy ions, in a sensitive region of a satellite instrument can damage the logic circuits and upset computer memories or control mechanisms. This effect is known as a Single Event Upset (SEU). The Microelectronics Package on board the CRRES mission was designed to study the SEU effects for a variety of chips. Solar Energetic Particles (SEP's) with energy between 10-500 MeV/nucleon are one source of SEU's. It is, therefore, important to model SEP events, in order to calculate the Linear Energy Transfer (LET) spectra needed for predicting the occurrence of SEU's. The solid state detector telescope ONR-604 /1/ on CRRES can measure heavy ions from helium (40-100 MeV/nucleon) to iron (185-500 MeV/nucleon). Heavy ions (neon and above) were analyzed with highest priority in the instrument and are called P1 particles.

Adams *et al.* /2/ determined the solar energetic heavy-ion fluxes by scaling from solar proton spectra and by utilizing a flare relative composition dataset measured at low energies. In a summary of SEP observations made by IMP-8 during 1973-83, Chenette and Dietrich /3/ pointed out that, for most SEP's, the spectra have a similar shape at energies 10-400 MeV/nucleon for the various ions heavier than boron. This result was confirmed at low energies (2-25 MeV/nucleon) by Reames *et al.* /4/, who showed that heavy ions and Helium have similar spectral shapes. However, the shape of the proton spectrum is usually different from that of the heavy ions /5/. Two different types of SEP events can be distinguished according to their heavy-ion content: "rich" and "normal" /2/. The heavy ion "rich" events tend to be impulsive events while "normal" events tend to be gradual in their onset time history /6/. In the following sections a SEP model is developed and applied to solar flares during the 1990/1991 CRRES mission.

MODELING SEP EVENTS

There are five steps in modeling a SEP event: (1) Determine the time-intensity profile including the start, peak and end of the SEP event. (2) Obtain peak and average fluxes for helium and protons and fit each to a power-law form:

$$dJ/dE = A(E/E_0)^{-\gamma}, \qquad (1)$$

where E_0 is a "representative energy" for each SEP event. The spectral index γ is assumed to be the same as the helium index for all the heavy elements. (3) Calculate the fluence (in particle/cm^2-sr-MeV/nucleon). (4) Find the heavy-ion enrichment parameter δ, defined /3/ as $\delta = (\ln(Fe/O) - \ln 0.155)/18$. where 0.155 is the mean solar corona Fe/O abundance ratio /7,8,9/. (5) Apply the δ parameter to scale the solar heavy-ion fluxes of different species from the solar helium spectra. Then the LET spectra can be calculated for various thicknesses of shielding.

THE OBSERVATIONS

Helium: Time Histories

From the helium counting rates, a total of 26 SEP events have been identified during the CRRES mission, of which the March and June, 1991 events are the largest. The 12 major SEP events, with peak helium counts per orbit > 100, are tabulated in Table 1, and each SEP event is associated with a specific solar flare. Table 1 also lists the start, peak and end time at Earth of each SEP event. The SEP particles are believed to be accelerated to energies of tens to hundreds of MeV/nucleon by a shock wave and then move outward through the corona and diffuse along the magnetic field lines into interplanetary space. Therefore, although a solar flare event lasts seconds to hours, as observed in the H_α line, X-ray, Gamma-ray, and radio spectral regions, a SEP event at Earth can last from hours to more than a week, with a typical period of 2-3 days.

TABLE 1. Major SEP Events During the CRRES Mission

Event Number	Peak Orbit	Start (Day)	Peak (Day)	End (Day)	Peak He (cnt/orb)	P1/He (10^{-4})	Assoc. Flare (Day/UT)
1	451	26.0	27.2	29.3	201	-	Jan 25/0630
2	462	31.3	31.7	32.4	481	-	Jan 31/0230
3	522	56.4	56.5	57.6	235	-	Feb 25/0819
4	586	82.1	82.6	84.0	10000	9±2	Mar 22/2247
5	593	84.6	85.4	87.6	3234	-	Mar 24/2046
6	710	133.1	133.4	135.0	517	-	May 13/0144
7	774	153.0	159.6	162.1	23404	1.7±0.5	Jun 04/0352
8	783	162.1	163.4	165.5	19135	2.9±0.7	Jun 11/0209
9	792	166.3	167.2	173.6	11918	10±2	Jun 15/0821
10	829	179.5	183.0	188.3	1648	-	Jun 28/0626
11	842	188.4	188.6	190.3	450	-	Jul 07/0223
12	961	238.7	239.7	241.4	156	-	Aug 25/0115

The March and June events have helium counting rates that increase two orders in magnitude, and these events, 4 and 7 in Table 1, are used as examples to illustrate the model. The time-intensity profiles of these two SEP periods are plotted in Figure 1a. The peak helium fluxes occurred at orbit 586 for the March event and at orbits 774, 783, and 792 for the June events. These multiple peaks in the SEP events are actually associated with different particle injections, as listed in Table 1. The March event includes two major solar flares and the June period contains at least three large solar flares.

The CRRES satellite was in a geosynchronous transfer orbit (GTO) and traveled through the magnetosphere from a perigee of ~ 350 km to an apogee of ~ 33,580 km with an inclination of 18.2 degrees. Helium with different energies observed at various positions in the orbit (i.e., different L shells) will experience different geomagnetic cutoff effects. Figure 1b displays the helium counting rate as a function of L shell for orbits 586 (top) and 774 (bottom). Helium above 40 MeV/nucleon can freely access L > 5, in agreement with the transmission function calculations. In addition, most helium is detected at L > 6 since the spacecraft spends the most time at high L shells.

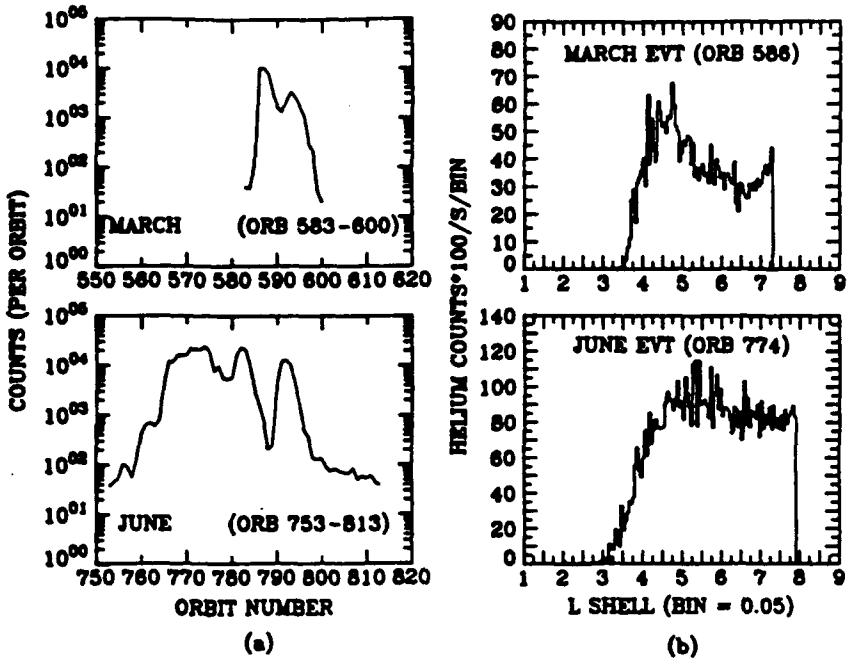

Fig. 1. (a) Time-intensity profiles for the March (top) and June periods (bottom). Multiple peaks in the profiles are associated with different solar flares. (b) Helium rate as a function of L shell for orbits 586 (top) and 774 (bottom). Each bin is 0.05 L unit.

Helium: Energy Spectra and Fluence

The helium (L > 6) energy spectra (after corrections for the geometry factor of the instrument and the detector efficiency) are shown in Figure 2 for the peak flux orbits 586 and 774. The ONR-604 energy range for helium is 45-90 MeV/nucleon, and E_0 has been chosen as 66 MeV/nucleon. The two solid lines are the least-squares fit to equation (1) which is an excellent representation of the observed data. The spectral index γ is the most important parameter and is listed in column 3 of Table 2. The peak spectral amplitude A^p_{He}, listed in column 2, is the peak helium flux at energy E_0. Also given are the spectral index and amplitude, denoted as γ^a and A^a_{He}, for the duration of each SEP event, with A^a_{He} again the average flux at energy E_0. The estimated errors for both spectral index and amplitude are from least-squares fitting.

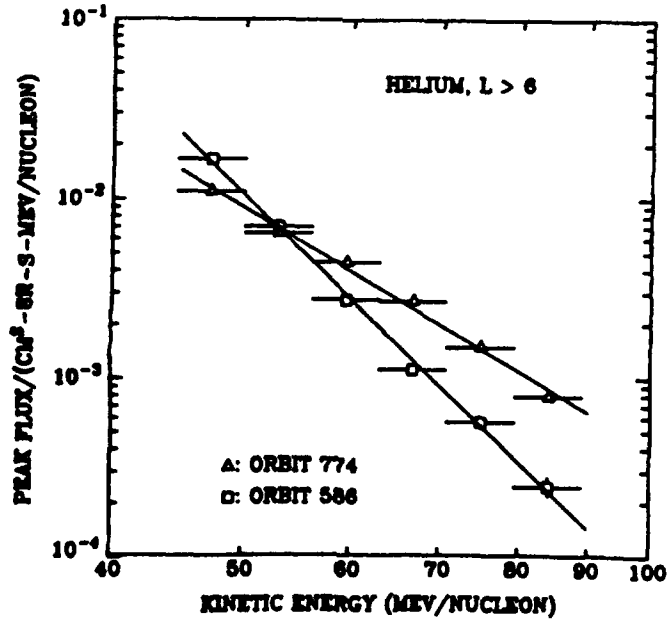

Fig. 2. Helium energy spectra at L > 6 for orbits 586 (square) and 774 (triangle). The straight lines are the least-squares fit to Eq. (1).

The average fluence. column 6 of Table 2. is simply the product of the average flux and the duration, which represents the intensity of a SEP event. another important parameter in the model.

TABLE 2. Helium Spectrum and SEP Model Parameters

Event	Peak Spectra A^p_{He}*	γ^p	Average Spectra A^a_{He}*	γ^a	Fluence** (at E_0)	Duration (Days)	$F\epsilon/O$	δ
March (4)	13.9±0.5	7.3±0.2	10.7±0.5	6.8±0.2	175.7×10^4	1.9	4.37	0.186
June (7)	26±1	4.5±0.2	9.6±0.4	4.3±0.2	754.8×10^4	9.1	0.098	-0.025

* in particles/m^2-sr-s-MeV/nucleon: ** in particles/m^2-sr-MeV/nucleon.

Heavy-Ion Content

Since the collecting power of ONR-604 is not sufficient to obtain enough heavy ions at the energies sampled by the instrument, it is difficult to obtain an $F\epsilon/O$ ratio directly for the SEP events. Therefore. the ratio of P1 to helium is used as an indicator of the SEP heavy-ion enrichment. The P1 particles contain heavy ions from neon to nickel with the dominant elements being magnesium. silicon and iron. Due to the steep spectra of SEP ions and to the high energy detection ranges of ONR-604. we expect to be able to detect P1 particles only from the largest solar flares. Figure 3 illustrates the heavy-ion content for 200 orbits around the June events. The top panel is the P1 counts/orbit, middle panel is the helium counts/orbit, and the bottom panel is the ratio, $P1/He$. The P1 rate usually peaks one or two orbits before that of helium. Figure 3 also shows that the P1/He ratio during quiet times (i.e., galactic cosmic rays) is much higher than during solar flares. For each of the four largest SEP events we calculated the upper-limit of the P1/He ratio (since no subtraction of the GCR background from the P1 flux was made) by averaging over four consecutive orbits for the event. The results are tabulated in column 7 of Table 1.

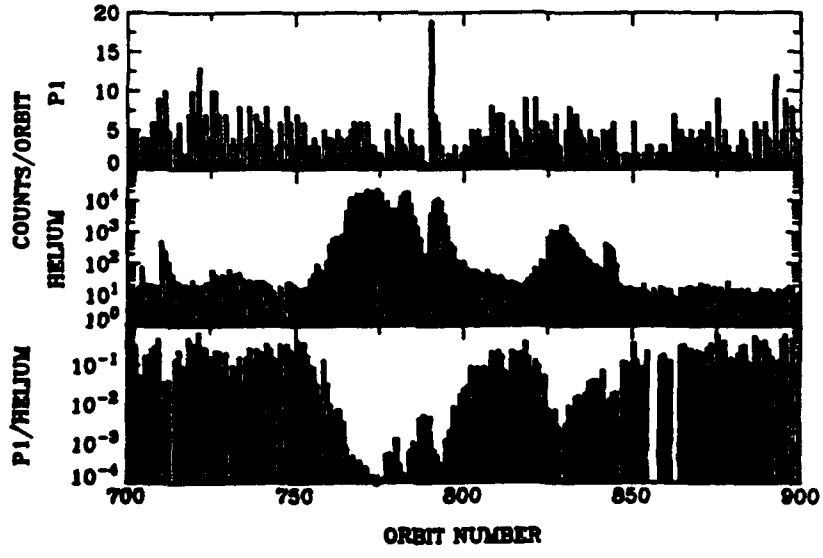

Fig. 3. Heavy-ion content for 200 orbits around the June events. The top panel is the P1, and the middle panel the helium in counts per orbit, and the bottom panel shows the ratio between them. P1 contains heavy ions from ~ neon to nickel.

It is noted that the energy range of P1 (100-500 MeV/nucleon) is different from that of helium (45-90 MeV/nucleon) and that the detector efficiency varies for different SEP events as well as for different ion species. The ratio of P1 to He after correcting for the energy range and instrument efficiency is $(P1/He)_0 = c(P1/He)$ where c is the correction factor and $(P1/He)$ is the observed value listed in Table 1. The $(F\epsilon/O)$ ratio is then obtained through

$$F\epsilon/O = (F\epsilon/P1)(P1/He)_0(He/O), \quad (2)$$

where $He/O \sim 55.2$ for SEP's /8.9/ being independent of the energy /10/ and $Fe/P1 = 0.192$ and 0.370 for heavy-ion "normal" and "rich" flares, respectively /2/. For events 4 and 7 the factor c is estimated to be 238 and 54, respectively. The corresponding Fe/O ratios and δ values are summarized in Table 2. For comparison, the average value of the Fe/O is 1.0 for heavy-ion "rich" events and 0.155 for "normal" events /11/, observed at lower energies (< 10 MeV/nucleon). This ratio can vary by several orders of magnitude at higher energies from flare to flare.

Compared to the variations of other ion abundances, the ratio He/O does not vary much for different SEP events /10/. It is therefore possible to scale the fluxes of different heavy-ion species directly from that of helium instead of oxygen /3/ through

$$A_X = (A_{He}/55.2)\,(X/O)_{SEP}\,e^{\delta(Z_X-8)}, \qquad (3)$$

where X represents a specific heavy-ion element, Z_X its charge, and $(X/O)_{SEP}$ the X/O abundance ratio for "normal" SEP (i.e. solar corona) matter. Figure 4 plots the predicted spectra for oxygen and iron. The March flare is a heavy-ion "rich" case with the spectral amplitudes for oxygen and iron $A_O = 2.5 \times 10^{-5}$ and $A_{Fe} = 1.1 \times 10^{-4}$ (cm^2-sr-s-MeV/nucleon)$^{-1}$, respectively. Orbit 774 (event 7 in Table 1) is a heavy-ion "normal" case, and its predicted oxygen and iron spectra (Fig. 4b) have $A_O = 4.7 \times 10^{-5}$ and $A_{Fe} = 4.6 \times 10^{-6}$ (cm^2-sr-s-MeV/nucleon)$^{-1}$. It is interesting to note that event 4 corresponds to an impulsive helium time-intensity profile with only 0.5 days from start to peak, while event 7 has a gradual helium time profile with more than 6.5 days from start to peak (Table 1). Such a correspondence between heavy ion content and flare time history has been seen in other events /6/.

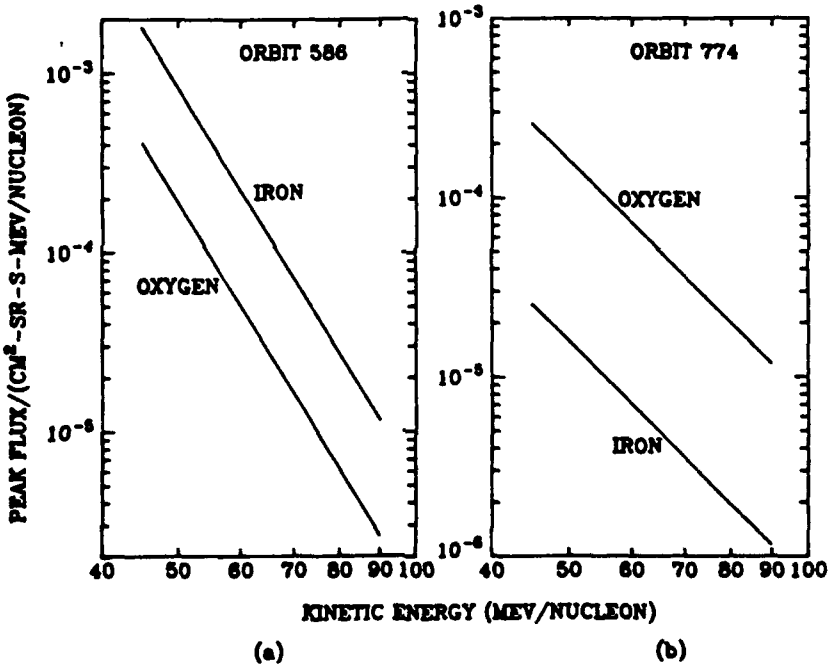

Fig. 4. Predicted energy spectra for oxygen and iron scaled from the solar helium fluxes for orbits 586 (a) and 774 (b).

The proton data, supplied by National Geophysical Data Center, are from the geosynchronous GOES-7 satellite and cover an energy range of 15-500 MeV. The power-law spectrum assumed in the SEP model is also a good representation for the protons. The inferred proton spectral parameters for events 4 an 7 are $A = 2.7 \pm 0.9$ and 0.22 ± 0.04 particles/cm^2-sr-s-MeV/nucleon and $\gamma = 4.7 \pm 0.4$ and 3.1 ± 0.2. It is noted that the proton spectral indices are significantly different from that of helium, which may be due to the charge/mass ratio difference between these two species. Therefore, scaling from proton spectra is not an accurate method to predict heavy-ion fluxes.

SUMMARY

Solar energetic particle events can be separated into two groups according to their heavy-ion content. The 1991 March SEP event is heavy-ion "rich" and is associated with an impulsive solar

flare. while the first event in June 1991 is "normal" and is associated with a gradual type flare. It is found that the solar proton spectral indices are different from that of helium. The solar heavy-ion spectra can be obtained by employing the enrichment parameter δ and by scaling from the solar helium spectrum. The SEP model developed here provides a good representation of the observations made by ONR-604 and GOES-7 for the energy range 45-90 MeV/nucleon for helium and 15-500 MeV for protons. The model can be generalized into a predictive tool for calculating the heavy-ion fluxes, LET spectra and SEU rates of space instruments during solar flares.

ACKNOWLEDGEMENT

Research was supported by NASA Contracts NAGW 2368 and NAG 5-706, Air Force Contracts F 19628-90-K-0025, -0026, and -C-0101 and ONR Contract N00014-90-J-1466.

REFERENCES

1. J. A. Simpson, M. G. Munoz, M. Perkins, and J. P. Wefel. The Experiment for High Energy, Heavy Nuclei Composition (ONR-604), in *CRRES/SPACERAD Experiment Descriptions*, eds. M. S. Gussenhoven, E. G. Mullen and R. C. Sagalyn, Air Force Geophysics Laboratory Report AFGL-TR-85-0017 (Hanscom AFB, MA), p. 163 (1985).

2. J. H. Adams, Jr., R. Silberberg, and C. H. Tsao. Cosmic Ray Effects on Microelectronics, Part I: The Near-Earth Particle Environment. NRL Memorandum Report 4506. NRL, Washington, DC, USA (1981).

3. D. L. Chenette and W. F. Dietrich. The Solar Flare Heavy Ion Environment for Single-Event Upsets: A Summary of Observations Over the Last Solar Cycle, 1973-1983, *IEEE Trans. Nuc. Sci.*, Vol. NS-31, (6), 1217 (1984).

4. D. V. Reames, I. G. Richardson, and K. P. Wenzel. Energy Spectra of Ions from Impulsive Solar Flares, *Ap.J.*, **387**, 715 (1992).

5. R. E. McGuire, T. T. von Rosenvinge, and F. B. McDonald. The Composition of Solar Energetic Particles, *Ap.J.*, **301**, 938 (1986).

6. D. V. Reames. Energetic Particles from Impulsive Solar Flares, *Ap.J. Suppl.*, **73**, 235 (1990).

7. H. H. Breneman and E. C. Stone. Solar Corona and Photospheric Abundances from Solar Energetic Particle Measurements. *Ap.J.(Letters)*, **299**, L57 (1985).

8. H. V. Cane, D. V. Reames, and T. T. von Rosenvinge. Solar Particle Abundances at Energies of Greater Than 1 MeV Per Nucleon and the Role of Interplanetary Shocks. *Ap.J.*, **373**, 675 (1991).

9. D. V. Reames, I. G. Richardson, and L. M. Barbier, On the Differences in Element Abundances of Energetic Ions from Corotating Events and from Large Solar Events, *Ap.J.(Letters)*, **382**, L43 (1991).

10. J. E. Mazur, G. M. Mason, B. Klecker, and R. E. McGuire, The Energy Spectra of Solar Flare Hydrogen, Helium, Oxygen, and Iron: Evidence for Stochastic Acceleration. *Ap.J.*, (in press) (1992).

11. D. V. Reames. Energetic Particle Observations and the Abundances of Elements in the Solar Corona, in 1st SOHO Workshop, Annapolis, MD (1992).

The LET Spectrum and Its Uncertainty During the CRRES Mission

D.L. Chenette*, T.G. Guzik**, and J.P. Wefel**

*Space Sciences Laboratory, O/91-20, B/255, Lockheed Palo Alto Research Laboratory, 3251 Hanover Street, Palo Alto, CA 94304, USA **Department of Physics and Astronomy, 277 Nicholson Hall, Louisiana State University, Baton Rouge, LA 70803

ABSTRACT

We present Linear Energy Transfer (LET) spectra calculated for the 1990-1991 CRRES mission using the galactic cosmic ray (GCR) and solar energetic particle (SEP) models developed for the CRRES/SPACERAD program and presented by Chen, *et al.* 1992 at this conference /1,2/. We discuss how the spectra vary with changes in the galactic cosmic ray and solar energetic particle models. Finally, we illustrate the application and significance of these results by using them to predict single event upset event rates in a sample integrated circuit memory device, a 256 x 4-bit bipolar static RAM (93L422).

INTRODUCTION

The Linear-Energy Transfer (LET) spectrum provides the flux of energetic ions as a function of the energy deposited per unit distance (LET) in a medium. This spectrum describes the radiation source for studies of effects due to single-ion interactions like Single-Event Upsets (SEU) /3/.

Models of the space radiation environment and laboratory test and design analysis tools have been developed for guiding the engineering of space systems to minimize SEU effects /4,5,6/. A number of experiments have been performed in space to validate these models and methods /7,8/. The CRRES/SPACERAD program includes on-orbit SEU tests of many different microelectronic devices in the CRRES Microelectronics Package /9,10/. In support of this program we have developed improved models of the radiation environment mission based on contemporary measurements of both the galactic cosmic ray and solar energetic ion fluxes.

In this paper we describe the methods used to convert the galactic cosmic ray and solar energetic ion flux measurements into LET spectra and present the LET spectra resulting from the particle flux spectra presented in the companion papers /1,2/. These include LET spectra for the omni-present galactic cosmic ray flux as well as for a pair of large solar energetic particle events. Finally we provide some SEU rate estimates for a specific bipolar memory device, the 93L422, a 256 x 4-bit static RAM.

LET SPECTRUM CALCULATION METHOD AND COMPARISON

We calculate LET spectra behind a specified thickness of shielding using differences of the range function, R(E,Z,M), for an ion with kinetic energy E, atomic number Z and mass M. The range function is scaled from the proton range tabulation of Janni /11/ at ion energy E/M by MZ^{-2}. A range extension correction is applied to account for the ion charge state at low velocities based on the results of Heckman, *et al.* /12/. The effects of nuclear interactions are not included in this calculation. For thick shields, when the effects of these interactions become important, this LET spectrum will over-estimate the real spectrum at high LET and underestimate the real spectrum at low LET.

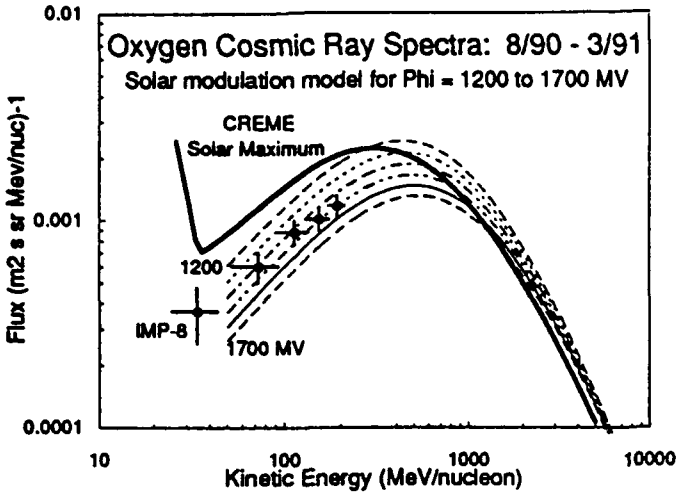

Figure 1. A comparison of measurements and models of the galactic cosmic ray oxygen flux in the interplanetary medium near earth in late 1990 and early 1991. The points labeled "IMP-8" are from The University of Chicago cosmic ray instrument aboard the IMP-8 satellite. The dashed lines are the results of our solar modulation model calculation for a range of the solar modulation parameter (F) chosen to fit the measurements. The heavy solid line is the oxygen spectrum for solar maximum conditions from the CREME model /5/.

Above an LET corresponding to the maximum for iron the spectra are more speculative because the available measurements are scarce. For ions above nickel (Z=28) the CRRES model uses the iron spectrum scaled by the relative composition provided by Cameron /13/.

GCR SPECTRA FOR CRRES

As described in the companion papers /1,2/, the GRC model used in this work is based on a model of galactic cosmic ray spectra in the local interstellar medium together with a calculation to transport the galactic cosmic rays to earth orbit under the influence of solar modulation. The local interstellar spectra change only on time scales comparable to the mean age of the cosmic rays (~10^7 years /14/).

With an adequate model for solar modulation the entire history of measurements of galactic cosmic ray composition and energy spectra can be accommodated by the proper choice of local interstellar spectrum. All of the local temporal variation can be attributed to solar modulation with its known dependence on mass, charge, and energy. Predicted flux spectra for all ion species thus can be obtained self-consistently using this method from only a few measurements. An example is shown in Figure 1, where the spectrum of galactic cosmic ray oxygen as measured in the interplanetary medium near earth from August 1990 through March 1991 is compared to results of our solar modulation model (as well as to the CREME solar maximum spectrum /5/). The best-fit value of the solar modulation parameter (Φ) for the measured oxygen spectrum is Φ = 1444 ± 42 MV. The uncertainty quoted is the formal error of the fit based on a chi-square distribution. Due to the paucity of data this probably underestimates the true accuracy of the result.

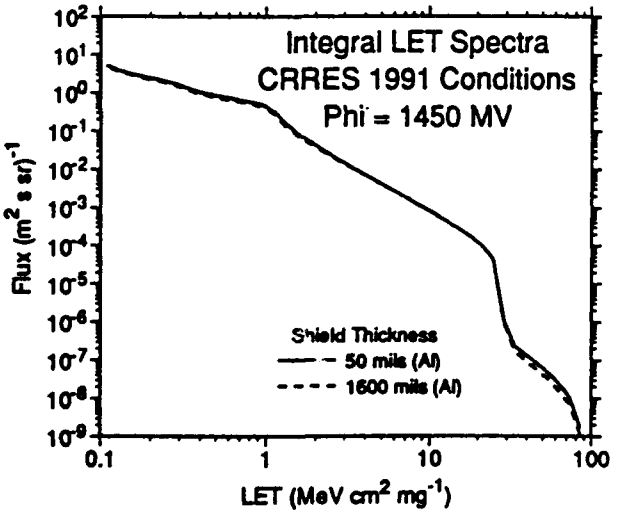

Figure 2: The LET spectrum calculated for the period August 1990 through March 1991. This spectrum is appropriate for periods without significant solar energetic particle fluxes during the early part of the CRRES mission.

The solar modulation level inferred from Figure 1 is near the maximum for the solar cycle. In addition, neutron monitor records indicate that the intensity of the galactic cosmic ray flux in this solar maximum is lower than at any time since 1960. LET spectra calculated for this maximum solar modulation level are shown in Figure 2. Spectra were calculated for shield thicknesses ranging from 50 to 1600 mils of aluminum. The limiting spectra for this range are indicated in the graph. The LET spectrum is not strongly dependent on the thickness of shielding over this range, especially at lower LET values, because the galactic cosmic ray spectrum peaks at several hundred MeV/nucleon (Figure 1). At LETs above ~30 MeV cm^2 mg^{-1}, where only ions heavier than iron can contribute to the spectrum, the particle range corresponding to the peak of the cosmic ray spectrum is several hundred mils of aluminum. Thus thicker shielding can reduce the flux due to these high

LET particles. Lower LET particles have longer ranges in material. Thus shields up to the thicknesses considered here have little effect on the total flux at lower LET.

Using our solar modulation model we can quantify the solar-cycle dependence of the LET spectrum on the solar modulation level. Figure 3 shows the calculated range of variation of LET spectra between solar minimum (Φ = 450 MV) and solar maximum (Φ = 1450 MV) conditions for various thicknesses of shielding from 50 to 1600 mils of aluminum. For thinner shields and at larger LETs the variation can be over a factor of 6. These effects are due to the range-energy and energy spectrum relationships discussed with Figure 2.

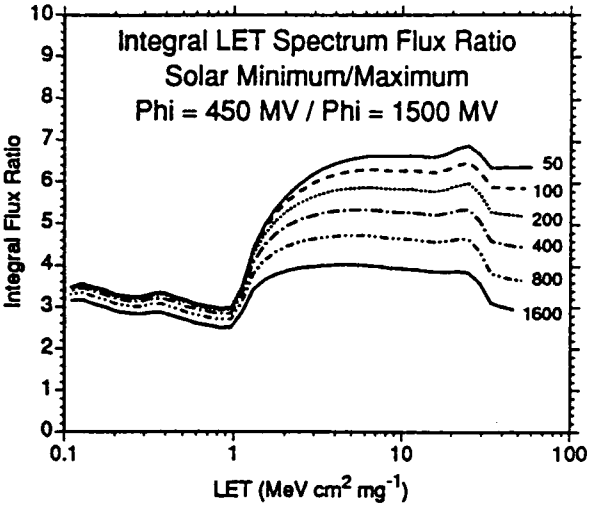

Figure 3 The ratio of LET spectra based on the CRRES/SPACERAD models between solar minimum and solar maximum. At solar minimum the LET spectrum is about 3 times higher than the solar maximum spectrum for low LETs. The ratio increases to a factor of 6 - 7 for thinner shields at high LETs.

Effects of smaller variations in the level of modulation have been investigated also. Near solar maximum (e.g. 1991), the change in LET spectrum intensity due to a change in the level of solar modulation is similar to the shape evident in Figure 3. For LET <1 MeV cm^2 mg^{-1} a change in modulation level of 100 MV produces a change in LET spectrum of -8% to -10% for shields of 50 to 1600 mils aluminum. Increasing the modulation level reduces the flux, and a larger variation is observed at the thinner shield thicknesses. Between about 2 and 30 MeV cm^2 mg^{-1} a 100 MV change in modulation level produces a -13% to -15% change in the LET spectrum, depending on shield thickness.

SEP LET SPECTRA

Chen, *et al.* /2/ discussed two of the largest solar energetic particle (SEP) events observed during the CRRES mission. The flare of 22 March 1991 was "iron rich" and had the highest peak heavy ion intensity at low energy, but this event also had a very steep energy spectrum with little flux enhancement over the galactic cosmic ray component at high energy. The flare of 4 June 1991 had a smaller peak intensity, but was in an extended series of overlapping flare events which accumulated a large total fluence. For both events the composition inferred is an event average.

Total LET spectra for these two events are shown in Figure 4 for several different shield thicknesses. The galactic cosmic ray LET spectrum is from Figure 2. The solar flare LET spectra shown in Figure 4 correspond to the peak flux intensities inferred for each event. For estimating event-integral effects these flux spectra

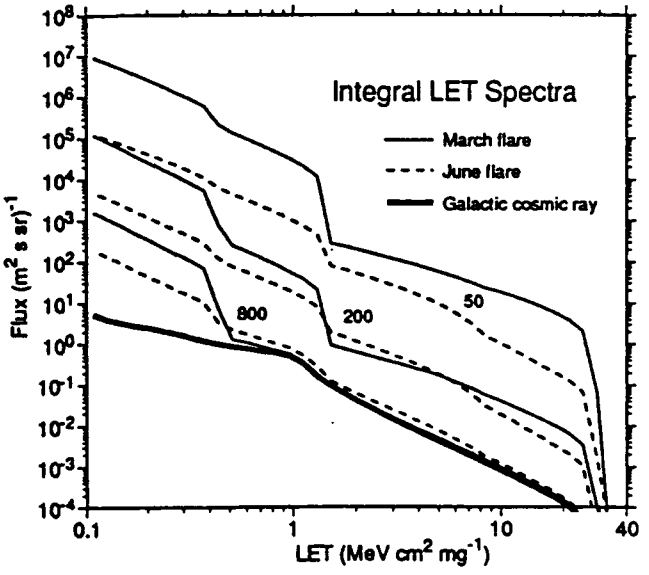

Figure 4: Integral LET spectra for the solar flares of March (solid line) and June 1991 (dashed line) are compared to the galactic cosmic ray LET spectrum (thick line). The flare LET spectra are presented for shield thicknesses corresponding to 50, 200, and 800 mils of aluminum.

Table 1. Single Event Upset Rate Estimates for a 256 x 4-bit Bipolar Static RAM (93L422)

Environment	Single-Event Upsets per Device (1024 bits) 50 mil (Al) shield	1600 mil (Al) shield
Solar maximum (Φ = 1500 MV)	0.11 per day	0.10 per day
1990-1991 CRRES (Φ=1444 MV)	0.12 per day	0.11 per day
Solar minimum (Φ = 450 MV)	0.41 per day	0.30 per day
4 June 1991 SEP event peak	35 per hour	0.15 per day
22 March 1991 SEP event peak	3 per second	0.16 per day
4 June 1991 SEP total fluence	2.8×10^3 total	0.14 SEP+1.0 GCR*
22 March 1991 SEP total fluence	3.5×10^4 total	0.007 SEP+0.2 GCR*

*At this shield thickness, most of the SEU events during the flares are from the GCR component.

can be converted to fluence spectra using time constants inferred from the companion paper /2/. These constants are 1.45 days for the March event and 3.36 days for the June event. Other details of the source particle spectra models are provided in the other paper.

These flares were large, with total fluences which placed them in the upper few percent of the 1973 - 1984 heavy ion fluence distributions presented by Chenette and Dietrick in /15/. Because the solar flare particle flux intensities decrease rapidly with increasing energy, the variation in the intensity of the LET spectrum with shielding is very strong. Additionally, however, the very steep energy spectrum of the March event (power-law energy spectral index of -7.3) placed this event in the quartile of the smallest flares observed from 1973 - 1984 in terms of the total heavy ion fluence for energies over 100 MeV/nucleon.

SINGLE EVENT UPSET RATE ESTIMATES

To illustrate the use of the LET spectra presented here we provide calculations of the expected upset rate in a 256 x 4-bit bipolar static memory device, part number 93L422. This device has been characterized well in ground-based accelerator tests and was used in a space-based validation study /8/. The measured single-event upset cross-section of this device is provided in /8/ together with a discussion of the device geometry and related issues. The Fairchild version of this part was used in the calculations presented here. At large LET values the upset cross-section of this part is just over 10^{-5} cm^2 per bit, or 10^{-2} cm^2 per device.

The upset rate calculations were performed using the methods of Chenette et al. /16/, which take into account the measured shape of the upset cross-section as a function of effective LET. The results are presented in Table 1. Extreme lower and upper limit bounds surrounding the results shown in the table are typically within about 50% of the tabulated value. These limits are extreme limits of the integration of the cross-section as measured in ground-based accelerator tests. The estimated numerical and measurement error of the procedure used to estimate these upset rates is smaller than these limits.

SUMMARY

LET spectra have been presented to describe the interplanetary heavy ion environment due to galactic cosmic rays and solar energetic particle events during the CRRES mission in 1990 and 1991. These spectra were based on the galactic cosmic ray and solar energetic particle models developed for the CRRES/SPACERAD program and presented by Chen, *et al.* 1992 at this conference /1,2/. For solar minimum conditions, these LET spectra are within 30% of the CREME results /5/. However, the galactic cosmic ray oxygen spectrum for the period August 1990 to March 1991 is significantly lower than the solar maximum spectrum of the CREME model. As a result, CREME will over-estimate the expected upset rate during these times. LET spectra for a large, heavy-ion rich, but high-energy poor solar particle event (22 March 1991) and

a large solar particle event with more typical composition and energy spectrum (4 June 1991) were presented and compared. Predicted single-event upset rates for a bipolar 256 x 4-bit static memory ranged from about 40 per year during solar maximum conditions when no solar energetic particle fluxes were present to about 3 per second for very thinly shielded parts at the peak of the 22 March event.

ACKNOWLEDGEMENTS

We thank Dr. M. Garcia-Muñoz of The University of Chicago for the IMP-8 oxygen spectra and Drs. W.A. Kolasinski and R. Koga of The Aerospace Corporation for the 93L422 upset cross-sections. This work was supported by the USAF Electronic Systems Division under contract F19628-90-C-0101.

REFERENCES

1. J. Chen, D. Chenette, R. Clark, M. Garcia-Muñoz, T.G. Guzik, K. Pyle, Y. Sang, and J. Wefel, 29th Plenary Meeting of COSPAR, paper F2.6-M1.07, 1992.

2. J. Chen, D. Chenette, G. Guzik, M. Garcia-Muñoz, K. Pyle, Y. Sang, and J. Wefel, 29th Plenary Meeting of COSPAR, paper F2.5-M2.11, 1992.

3. D. Binder, E.C. Smith, and A.B. Holman, *IEEE Trans. Nuc. Sci.*, NS-22, 2675, December 1975.

4. J.C. Pickel and J.T. Blandford, *IEEE Trans. Nuc. Sci.*, NS-27, 1006, April 1980.

5. J.H. Adams, R. Silberberg, and C.H. Tsao, "Cosmic Ray Effects on Microelectronics, Part I: The Near-Earth Particle Environment", NRL Memorandum Report 4506, Naval Research Laboratory, Washington, D.C., 1981.

6. R. Koga, W.A. Kolasinski, J.V. Osborn, J.H. Elder, and R. Chitty, *IEEE Trans. Nuc. Sci.*, NS-35, 1638, December 1988.

7. J.B. Blake and R. Mandel, *IEEE Trans. Nuc. Sci.*, NS-33, 1616, December 1986.

8. M. Shoga, P. Adams, D.L. Chenette, R. Koga, and E.C. Smith, *IEEE Trans. Nuc. Sci.*, NS-31, 1217, December 1987.

9. K.P. Ray and E.G. Mullen, Pre-launch Data for the GL-701-1A Microelectronics Package, PL-TR-91-2007, Phillips Laboratory, Air Force Systems Command, Hanscom AFB, MA, 1991.

10. E.G. Mullen and K.P. Ray, 29th Plenary Meeting of COSPAR, paper F2.6-M2.03, 1992.

11. J.H. Janni, *Atomic Data and Nuclear Data Tables*, 27, July/September 1982.

12. H.H. Heckman, B.L. Perkins, W.G. Simon, F.M. Smith, and W.H. Barkas, *Physical Review*, 117, 544, 1960.

13. A.G.W. Cameron, in: *Essays in Nuclear Astrophysics*, ed. Barnes, Clayton, and Schramm, University of Cambridge Press, Cambridge, 1982, pp. 23-43.

14. J.A. Simpson, *Ann.Rev. Nucl. Part. Sci.*, 33, 323, 1981.

15. D.L. Chenette and W.F. Dietrich, *IEEE Trans. Nuc. Sci.*, NS-31, 1217, December 1984.

16. D.L. Chenette, T.L. Schumaker, and A.E. Williamson, An Accurate and Efficient Method to Calculate the Rate of Single Event Upsets from the LET Spectrum and SEU Cross Section Test Results, PL-TR-92-2084, Phillips Laboratory, Air Force Systems Command, Hanscom AFB, MA, 1992.